

AURORAL PLASMA WAVES

by

Donald A. Gurnett

January 1989

Department of Physics and Astronomy

The University of Iowa

Iowa City, IA 52242

\*Presented at the International Conference on Auroral Physics,  
Cambridge, England, July 11-15, 1988.

## ABSTRACT

This paper gives a review of auroral plasma wave phenomena, starting with the earliest ground-based observations and ending with the most recent satellite observations. Two types of waves are considered, electromagnetic and electrostatic. Electromagnetic waves include auroral kilometric radiation, auroral hiss, ELF noise bands, and low-frequency electric and magnetic noise. Electrostatic waves include upper hybrid resonance emissions, electron cyclotron waves, lower hybrid waves, ion cyclotron waves and broadband electrostatic noise. In each case, a brief overview is given describing the observations, the origin of the instability, and the role of the waves in the physics of the auroral acceleration region.

## INTRODUCTION

The study of auroral plasma waves has a long and interesting history extending over more than half a century. The first reported observation of a plasma wave phenomenon associated with the aurora was in 1933 by Burton and Boardman [1933]. Using a telephone receiver and a telegraph line as a simple receiving system, Burton and Boardman discovered that bursts of very-low-frequency (VLF) radio "static" were sometimes correlated with flashes of auroral light. Following this early discovery, little progress occurred for more than twenty years, until the International Geophysical Year (IGY), which started in 1957. Because of the interest in studying whistlers and other audio frequency radio phenomena during the IGY, many of the ground stations included VLF receiving equipment. Soon a substantial number of observations of auroral radio emissions became available. These observations clearly showed that radio emissions were often detected on the ground in association with auroral displays [Ellis, 1957; Duncan and Ellis; 1959; Dowden, 1959; Martin et al., 1960; Morozumi, 1963; Jorgensen and Ungstrup, 1962; Harang and Larsen, 1964]. Typically the emissions were the strongest in the VLF frequency range, from about 1 to 20 kHz. However, in some cases emissions were reported at frequencies as high as 500 kHz [Ellis, 1957]. Since the VLF auroral emissions tended to produce a hiss-like sound in the audio output of the receiver, these emissions soon became known as "auroral hiss." Among the early reports, Ellis [1957] has the distinction of being the first to propose a theory of auroral plasma waves. He suggested that the radio emissions were

produced by Cerenkov radiation from the precipitating charged particles responsible for the aurora. As will be discussed later, elements of his ideas still exist in modern theories of auroral hiss. For a more extensive review of the early ground-based observations, see Helliwell [1965].

The launch of the first Earth-orbiting satellites in the late 1950's opened an entirely new era in the study of magnetospheric plasma wave phenomena. The first satellite measurements of auroral plasma waves were reported by Gurnett and O'Brien [1964] using a VLF radio receiver on a low-altitude polar-orbiting satellite. These measurements clearly showed that auroral hiss is produced in regions of intense downgoing electron precipitation. Other later studies by Gurnett [1966], Hartz, [1970], Gurnett and Frank [1972] and Laaspere and Hoffman [1976] showed that auroral hiss is closely related to the occurrence of a beam-like electron precipitation event called an inverted-V [Frank and Ackerson, 1971]. Parallel electric fields caused by space charge regions at high altitudes over the auroral zone [Carlqvist and Bostrom, 1970] soon became the accepted mechanism for producing these electron beams.

During the late 1960's and early 1970's an entirely new type of high frequency auroral radio emission was detected by eccentric orbiting satellites. The first detection of this new radio emission was by Benediktov et al. [1965; 1968], using data from the Elektron 2 and 4 satellites. They identified bursts of radio noise at 725 kHz and 2.3 MHz at large distances from the Earth that were associated with geomagnetic storms. This same type of radio noise was also studied by Dunckel et al. [1970], at frequencies below 100 kHz, and

by Stone [1973] and Brown [1973], who showed that the peak intensity occurred between 100 to 500 kHz. A short time later, Gurnett [1974] demonstrated that the radiation was produced at high altitudes over the auroral regions in association with discrete auroral arcs. Gurnett also found that the total radiated power was very large, up to  $10^9$  Watts. The Earth was therefore found to be an intense planetary radio source, comparable in some respects to Jupiter, which had been known for many years to be an intense radio emitter [Burke and Franklin, 1955]. The radiation is now commonly called "auroral kilometric radiation" or "AKR," a term first suggested by Kurth et al. [1975].

Since these early observations, many additional types of auroral plasma waves have been discovered, most of which can be detected only by satellites in or above the ionosphere. In this chapter, we give an overview of the present state of knowledge of auroral plasma waves, with the main emphasis on results obtained in the last ten years. Although the early satellite investigations revealed the main types of auroral plasma waves, it is only recently, with the launch of the DE-1, EXOS-B, and Viking satellites, that measurements have been obtained in the critical altitude range from about 1 to  $3 R_E$  where the auroral acceleration occurs and many of the most intense waves are produced.

## PLASMA WAVE MODES

Before describing the observations, it is useful to first discuss the characteristic frequencies of a plasma and their relationship to the various wave modes that can exist in the auroral ionosphere. The most important characteristic frequencies of a plasma are the cyclotron frequency  $f_c$  and the plasma frequency  $f_p$ . As discussed by Stix [1962], a cyclotron frequency and a plasma frequency can be defined for each species. The cyclotron frequency for a charged particle of mass  $m_s$  and charge  $e_s$  is given by

$$f_{cs} = \frac{1}{2\pi} \frac{|e_s|B}{m_s}, \quad (1)$$

and the plasma frequency is given by

$$f_{ps} = \frac{1}{2\pi} \sqrt{\frac{n_s e_s^2}{m_s}} \quad (2)$$

where  $B$  is the magnetic field strength and  $n_s$  is the number density of the  $s$ th species.

To describe the modes of propagation that exist in a plasma, it is convenient to consider two classes of waves: electromagnetic and electrostatic. Electromagnetic waves have a magnetic field, whereas electrostatic waves do not. Usually, the propagation speed of electromagnetic waves is much higher than the thermal speed. For this reason, the propagation of electromagnetic waves can usually be

described by a model in which the plasma is completely cold (i.e., zero temperature). Electrostatic waves on the other hand almost always propagate at speeds on the order of the thermal speed. Therefore, thermal effects usually must be included in the analysis of electrostatic waves.

The approximate frequency ranges of the various electromagnetic modes of propagation that can exist in the auroral plasma are summarized in Figure 1. Two frequency regimes can be considered. At high frequencies, above the ion cyclotron frequencies, ion effects are generally not important. In this frequency range there are four separate electromagnetic modes of propagation [Ratcliffe, 1959]. These modes are shown in the top four panels of Figure 1 and are the free-space R-X mode, the free-space L-O mode, the Z mode, and the whistler mode. The term free space means that the mode reduces to the well-known free-space electromagnetic mode in the limit  $n_e = 0$  and  $B = 0$ . Using the terminology of Stix [1962], the R and L designations indicate the polarization with respect to the magnetic field (R for right, and L for left) and the O and X designations indicate the type of propagation perpendicular to the magnetic field (O for ordinary, and X for extraordinary). The Z mode is named after the so-called "Z trace" observed in ionograms [Ratcliffe, 1959], and the whistler mode is named after lightning-generated signals that propagate in this mode [Storey, 1953]. The L-O and R-X free-space modes have low frequency cutoffs at the electron plasma frequency,  $f_{pe}$ , and the R=O cutoff,  $f_{R=O} = f_{ce}/2 + [(f_{ce}/2)^2 + f_{pe}^2]^{1/2}$ . The Z mode is bounded at the upper limit by the upper hybrid resonance,  $f_{UHR} = [f_{ce}^2 + f_{pe}^2]^{1/2}$ , and at the lower limit by the L = O cutoff,

$f_{L=0} = -f_{ce}/2 + [(f_{ce}/2)^2 + f_{pe}^2]^{1/2}$ . The whistler mode has an upper frequency limit at  $f_{ce}$  or  $f_{pe}$ , whichever is lower.

At low frequencies, where ion effects are important, a new electromagnetic mode is introduced for each ion species. These modes are called electromagnetic ion cyclotron waves. The bottom two panels of Figure 1 show the electromagnetic ion cyclotron modes associated with  $H^+$  and  $O^+$ , which are the dominant ions in the auroral ionosphere. Other ion cyclotron modes also occur in association with various minor ions, such as  $He^+$ , but are not shown for simplicity. When two or more ion species are present, the ion cyclotron modes occur in distinct bands, one associated with each ion cyclotron frequency. The low frequency limit of each band is determined by a  $L=0$  cutoff. Polarization reversals and hybrid resonances also occur between each adjacent pair of ion cyclotron frequencies. For a discussion of these ion effects, see Smith and Brice [1964].

The electrostatic modes of propagation that can exist in the auroral plasma are summarized in Figure 2. These modes can be grouped in certain combinations, each associated with a characteristic type of resonance. First, there are the three hybrid modes, which occur at the upper hybrid resonance frequency,  $f_{UHR}$ , the lower hybrid resonance frequency,  $f_{LHR}$ , and the ion-ion hybrid resonance frequency,  $f_{IHR}$ . At these resonances the electromagnetic X-mode becomes purely electrostatic for propagation perpendicular to the magnetic field. Next there are the electrostatic electron cyclotron and ion cyclotron modes, also sometimes called the Bernstein modes. An electrostatic cyclotron mode occurs between each adjacent pair of cyclotron harmonics for each species in the plasma.

These modes are indicated by the dashed lines in Figure 2. The electrostatic cyclotron modes have wavelengths comparable to the cyclotron radius of the species involved, and disappear completely in the limit of zero temperature. Finally, there is the well-known electrostatic oscillation that occurs at the electron plasma frequency, also known as the Langmuir mode [Krall and Trivelpiece, 1973]. The Langmuir mode has a strong dependence on the electron temperature and degenerates to a monochromatic oscillation at the electron plasma frequency in the limit of zero temperature.

In addition to the modes associated with the ambient plasma, there are also a variety of electrostatic modes introduced when beams are present, the so-called "beam modes." A good example is the electron acoustic mode [Tokar and Gary, 1984], which only exists in the presence of an electron beam. For a review of the electrostatic beam modes, see Gary [1985].

To organize the presentation, the observations are described in the same order as in Figures 1 and 2, starting first with the electromagnetic modes, and proceeding to the electrostatic modes. In each section, the types of waves are described in order of decreasing frequency.

## ELECTROMAGNETIC WAVES

Auroral Kilometric Radiation.

The highest-frequency plasma wave emission generated in the auroral zone is auroral kilometric radiation (AKR). This radio emission typically has the highest intensities in the frequency range from about 50 to 400 kHz. A typical example of auroral kilometric radiation is illustrated in Figure 3, which shows a frequency-time spectrogram of an auroral kilometric radiation event detected during a DE-1 pass over the northern polar cap at a radial distance ranging from about 3 to 4  $R_E$ . The auroral kilometric radiation is the intense (dark) emission extending from about 80 to 400 kHz. The broadband electric field intensity of this radiation is very large, typically about 10 mV/m at a radial distance of 4  $R_E$ . The average power radiated from the Earth by the auroral kilometric radiation has been estimated by Gallagher and Gurnett [1979] to be about  $10^7$  to  $10^8$  Watts, although during intense events the peak power may be as high as  $10^9$  Watts [Gurnett, 1974]. The radiated power is highly variable, and often changes by up to 80 dB on time scales of ten minutes or less. The intensity variations are closely correlated with auroral magnetic disturbances [Benediktov, 1965, 1968; Dunckel et al., 1970; Voots et al., 1977], and with the occurrence of discrete auroral arcs [Gurnett, 1974; Kurth et al., 1975]. Considerable fine structure is also evident in the frequency spectrum, usually consisting of narrowband tones drifting upward and downward in frequency [Gurnett et al., 1979; Morioka et al., 1981; Benson et al., 1988].

Spatial intensity surveys [Gurnett, 1974; Gallagher and Gurnett, 1979] and direction-finding measurements [Kurth et al., 1975; Alexander and Kaiser, 1976] clearly established that the auroral kilometric radiation is generated along the nighttime auroral field lines at radial distances from about 2 to 4  $R_E$ . Observations show that the radiation is generated in a broad beam directed away from the Earth more or less as shown in Figure 4. High plasma densities in the lower levels of the ionosphere produce a propagation cutoff that prevents the radiation from reaching the ground. Polarization measurements by Shawhan and Gurnett [1982] and Mellott et al. [1984] using the DE-1 spacecraft show that the radiation is primarily generated in the R-X mode, although a small amount ( $\sim 2$  percent) of L-0 mode radiation is also present. A spectrogram showing the polarization during a typical DE-1 pass over the auroral zone is shown in Figure 5. The dark black region is right-hand polarized R-X mode radiation, and the white region is left-hand polarized L-0 mode radiation. The difference in the low frequency cutoff of the two modes is believed to be a propagation effect caused by differences in the refractive characteristics of the two modes. Usually, the R-X mode is refracted outward away from the Earth more strongly than the L-0 mode.

Several factors strongly indicate that both the L-0 and R-X mode radiation are generated close to the electron cyclotron frequency. The strongest evidence of this relationship comes from radio direction finding measurements and comparisons with auroral images. By using two-dimensional radio direction finding techniques, the direction of arrival of the auroral kilometric radiation can be

determined with a high degree of accuracy. If it is assumed that the radiation is generated at the electron cyclotron frequency, then the source position can be uniquely determined from the intersection of the direction of arrival and the surface defined by  $f = f_{ce}$ . Once the source position is known, the magnetic field line can be traced from the source down to the atmosphere and compared with auroral optical emissions. This process is illustrated in Figure 6, from Huff et al. [1988]. The points labeled 1 through 4 show the source positions determined at four frequencies, 104 kHz, 136 kHz, 170 kHz, and 218 kHz. The dashed lines then show the mapping of the magnetic field lines from these source positions down to an altitude of 200 km. As can be seen, the dashed lines all terminate in a region of bright auroral optical emissions. Similar results are found in many other examples. The close agreement confirms the basic assumption used in the analysis, namely that the radiation is generated very close to the electron cyclotron frequency.

The fact that the auroral kilometric radiation is generated at frequencies very close to the electron cyclotron frequency has several implications. As can be seen in Figure 1, the low frequency cutoff of the free space R-X mode is close to the electron cyclotron frequency only in regions where  $f_{pe} \ll f_{ce}$ . Since no radiation can be generated at frequencies below the cutoff frequency, the fact that the emission always occurs near  $f_{ce}$  implies that the condition  $f_{pe} \ll f_{ce}$  is a basic requirement for the generation of this radiation. The ionospheric plasma density therefore plays an important role in determining the bandwidth and conditions under which the radiation is generated.

Numerous theories have been proposed to explain the auroral kilometric radiation. For a review of some of the proposed theories, see Grabbe [1981]. At the present, it is widely believed that the radiation is produced by a Doppler-shifted cyclotron maser mechanism. Although some elements of this theory were first introduced by Melrose [1973], the first really detailed cyclotron maser theory of auroral kilometric radiation was developed by Wu and Lee [1979]. The main elements of Wu and Lee's theory are that the electrons interact with the waves via a Doppler-shifted cyclotron resonance interaction, and that the loss-cone in the auroral electron distribution provides the free energy source. By using a fully relativistic treatment of the cyclotron resonance interaction, Wu and Lee were able to show that the condition  $f_{pe} \ll f_{ce}$  arises as a direct result of the resonance condition. Thus, one of the basic generation conditions is readily explained by the theory. Numerous other investigators have since provided further refinements of the basic theory, including growth rate calculations [Omidi and Gurnett, 1982] and investigations of nonlinear and inhomogeneous effects [Wu et al., 1981; Winglee, 1985; Zarka et al., 1986]. Some uncertainty still exists concerning the free energy source. For example, Louarn et al. [1989] have recently suggested that electrons electrostatically trapped in the auroral acceleration region provide the primary free energy source. Despite uncertainties of this type, the main features of the cyclotron maser mechanism appear to be in good agreement with observations.

### Auroral Hiss and Z-Mode Radiation

Whistler-mode auroral hiss and Z-mode radiation are discussed together because they occur in overlapping frequency ranges and have somewhat similar characteristics. A spectrogram illustrating these two types of radio emissions is shown in Figure 7. This spectrogram is from a DE-1 pass over the nighttime auroral zone at a radial distance of about 3 to 4  $R_E$ . The auroral hiss is the broad intense emission extending from a few hundred Hz up to about 20 to 30 kHz. At low frequencies the emission is centered on the auroral zone, which is located from about 1232 to 1247 UT. At high frequencies the emission spreads out over a broad region, both toward the polar cap, and to a lesser extent toward the equator. The spreading at high frequencies produces a "funnel-shaped" frequency-time signature that is a characteristic feature of this radiation [Gurnett et al., 1983]. At high altitudes the auroral hiss often has a sharp high frequency cutoff. This cutoff can be seen in Figure 7, and is illustrated in greater detail in Figure 8, which shows a selected spectrum in which the cutoff is particularly sharp and well defined. The cutoff is a propagation effect that arises because the whistler mode has an upper frequency limit of either  $f_{pe}$  or  $f_{ce}$ , whichever is smaller. Since  $f_{pe}$  is typically less than  $f_{ce}$  at these altitudes, the cutoff is located at the electron plasma frequency,  $f_{pe}$ . The frequency range of the whistler mode is shown by the cross-hatched bar at the top of Figure 8.

Careful inspection of Figure 7 shows that an additional very weak emission exists above the upper cutoff of the auroral hiss. This emission is Z-mode radiation [Gurnett et al., 1983]. The Z mode

is unusual in that it is bounded at high frequencies by the upper hybrid resonance, and at low frequencies by the L=0 cutoff. Because of these cutoffs, Z-mode radiation is permanently trapped in the magnetosphere (see Figure 1). In most regions where the Z mode has been previously observed [Walsh et al., 1964; Gregory, 1969; Mosier et al., 1973], the electron plasma frequency is usually greater than the electron cyclotron frequency ( $f_{pe} \gg f_{ce}$ ). Under these conditions the Z mode is confined to a very narrow band around the electron plasma frequency. At high altitudes over the polar region, the opposite situation usually occurs, namely that  $f_{pe} \ll f_{ce}$ . Under these conditions the bandwidth of the Z mode becomes very large. The allowed frequency range of the Z mode is illustrated at the top of Figure 8 based on the known plasma parameters. As can be seen, the Z mode overlaps with the whistler mode. Since the auroral hiss is usually more intense than the Z mode, the lower part of the Z mode spectrum normally cannot be detected. Wideband spectrograms [Persoon and Gurnett, 1989] show that the Z mode is relatively smooth and continuous, very similar to auroral hiss. This is in strong contrast to the auroral kilometric radiation, which has considerable fine structure.

Several factors strongly indicate that auroral hiss is generated at wave normal angles near the resonance cone, where the index of refraction becomes infinite [Stix, 1962]. For wave normal angles near the resonance cone the whistler mode becomes quasi-electrostatic, with  $E \gg cB$ . The quasi-electrostatic characteristic explains why auroral hiss is easily detected by an electric antenna, but often not by a magnetic antenna. Resonance-cone propagation also

explains why auroral hiss seldom extends below the lower hybrid resonance frequency. As discussed by Stix [1962] the whistler mode resonance cone only exists for frequencies above the lower hybrid resonance frequency. Resonance-cone propagation also accounts for the tendency of the auroral hiss to spread out at high frequencies, thereby forming the funnel-shaped frequency-time spectrum. For this type of propagation, it can be shown that the radiation is emitted in a beam around the magnetic field with a beamwidth that increases with increasing frequency. As the spacecraft approaches the source field line, the higher frequencies are detected first, thereby producing the funnel-shaped spectrum [Gurnett et al., 1983].

Poynting flux measurements by Mosier and Gurnett [1969] show that auroral hiss propagates both upward and downward along the auroral field lines. At high altitudes, greater than 10,000 km, the radiation is usually propagating upward, and at low altitudes, less than 1000 km, the radiation is usually propagating downward, as shown in Figure 9. At intermediate altitudes both directions of propagation occur, although normally not on the same L-shell. At low altitudes the upward propagating emissions are usually very narrow, lasting only a few seconds. These upgoing low altitude emissions are sometimes called saucers [Gurnett and Frank, 1972; James, 1976]. Comparisons with low energy electron measurements clearly show that the downgoing auroral hiss is correlated with downgoing, 100 eV to 1 keV, "inverted-V" electron beams [Gurnett and Frank, 1972; Laaspere and Hoffman, 1976] and that the upgoing auroral hiss is correlated with upgoing,  $\sim 50$  eV, electron beams [Lin et al., 1984]. The fact that the electrons responsible for generating the radiation are

moving in the same direction as the wave, i.e.,  $\omega/k_{\parallel} = v_b$ , provides strong evidence that the radiation is produced by a Cerenkov interaction (also called a Landau resonance). Detailed calculations of whistler-mode growth rates have been performed by Maggs [1976] using realistic models for the auroral electron beams and a Landau resonance interaction. These calculations show good agreement with observed auroral hiss spectrums and intensities.

Although the understanding of auroral hiss is fairly advanced, relatively little work has been done on the propagation and generation of Z-mode radiation. Because of the broad bandwidth, the Z mode can propagate long distances both horizontally and vertically over the auroral zone and polar cap. The qualitative nature of this propagation is illustrated in Figure 10, which shows the "propagation window" formed by the propagation cutoff surfaces at  $f_{UHR}$  and  $f_{L=0}$ . At frequencies above  $f_{ce}$  the index of refraction surface has a resonance cone, so the propagation is highly anisotropic. At frequencies below  $f_{ce}$  the resonance cone disappears, and the propagation is more nearly line-of-sight, like free space. At low altitudes the radiation tends to be refracted away from the  $f_{L=0}$  surface, and once reflected asymptotically approaches the  $f_{ce}$  surface [Gurnett et al., 1983]. Because of the complicated propagation geometry it is difficult to accurately determine the source of the radiation. Most likely the source is located in the auroral zone, since this is where the largest intensities usually occur. Several generation mechanisms have been proposed. These include a beam-driven Landau resonance mechanism [Maggs and Lotko, 1981], a loss-cone driven cyclotron maser mechanism [Omidi et al., 1984], and mode

conversion from auroral hiss [Hashimoto et al., 1987]. Just which of these theories provides the best mechanism for generating the Z-mode radiation remains to be determined.

### ELF Noise Bands

Intense electromagnetic noise bands are frequently observed in the auroral zone by low altitude polar orbiting satellites at frequencies ranging from ten Hz to several hundred Hz. These emissions were first reported by Gurnett and Frank [1972], who called them ELF (extremely low frequency) noise bands. Gurnett and Frank also showed that they are closely correlated with regions of low energy, 100 eV to 10 keV, "inverted-V" auroral electron precipitation. A frequency-time spectrogram illustrating a typical example of this type of noise is shown in Figure 11. Similar signals are observed on both the electric and magnetic antennas, so the noise clearly consists of electromagnetic waves. Typical electric and magnetic field amplitudes are 3 to 10 mV/m and 10 to 30 pT. The bandwidth of the emission is quite narrow, usually less than 20 percent. Temerin and Lysak [1984] have shown that the center frequency decreases with increasing altitude, from a few hundred Hz at 1000 km, to a few tens of Hz at 10,000 km. The emission frequency is bounded by the proton cyclotron frequency and the helium cyclotron frequency. The electric field is polarized perpendicular to the electric field, and both left- and right-hand polarizations are observed.

Because the ELF noise bands always occur below the proton cyclotron frequency Temerin and Lysak [1984] suggested that the noise

is produced by electromagnetic ion cyclotron waves. The relevant ion cyclotron mode is the branch that exists between the proton cyclotron frequency,  $f_{cH^+}$ , and the helium cyclotron frequency,  $f_{cHe^+}$ . Once generated, the waves propagate downward as shown in Figure 12.

Reflection is believed to occur as soon as the ion hybrid resonance frequency,  $f_{IHR}$ , exceeds the wave frequency. Since the polarization reverses at the crossover frequency,  $f_x$ , both left- and right-hand polarized waves can occur, in agreement with the observations. The exact mechanism for generating these waves has not been firmly established. The most likely possibility appears to be a Landau resonance interaction with low energy electrons. In this case the free energy source would be the electron beam associated with the inverted-V electron precipitation.

#### Low-Frequency Electric and Magnetic Field Noise

For many years it has been known that intense low-frequency electric and magnetic field fluctuations are observed over the auroral zone by low-altitude polar-orbiting satellites. The electric field fluctuations were first reported by Heppner [1969] using double-probe electric field measurements on the OV1-10 spacecraft. This noise has been studied by many investigators, including Maynard and Heppner [1970], Kelley and Mozer [1972], Kintner [1976], Temerin [1978], Curtis et al. [1982] and Weimer et al. [1985]. Typically, the noise is most intense at frequencies below 1 Hz and decreases more or less monotonically with increasing frequency. A typical electric field spectrum is shown in Figure 13. Enhanced levels of magnetic field noise are also observed over the auroral zone by low-

altitude polar-orbiting satellites. These magnetic field fluctuations were first studied in detail by Armstrong and Zmuda [1973]. A typical magnetic field spectrum is shown in Figure 13. As can be seen, the general shapes of the electric and magnetic field spectrums are rather similar. Usually the magnetic field spectrum is steeper than the electric field spectrum, particularly at frequencies above 10 Hz. Typical power law spectral indices are -2.0 to -4.0 for the electric field, and -3.0 to -5.0 for the magnetic field. Both the electric and magnetic fields are perpendicular to the static magnetic field.

The initial interpretation of these observations was that the fluctuations are caused by independent quasi-static fields. The electric fields were believed to be produced by turbulent convective motions of the ionosphere [Kelley and Kintner, 1978], and the magnetic fields were believed to be produced by field-aligned currents [Armstrong and Zmuda, 1973]. However, more recently it was shown that the electric and magnetic field fluctuations are closely correlated [Smiddy et al., 1980; Gurnett et al., 1984]. Correlation coefficients are often as high as 80% at frequencies below 10 Hz, decreasing somewhat towards higher frequencies. The phase of the correlation is such that the Poynting flux is directed toward the Earth. The net energy flow integrated over the auroral zone is substantial,  $\sim 10^8$  Watts [Gurnett et al., 1984].

Two extreme views have been advanced to explain the origin of this noise. The first model, described by Smiddy et al. [1980], assumes that the fluctuations are caused by the motion of the spacecraft through a system of static field-aligned current

structures imbedded in the ionosphere. The electric fields are generated by the closure of the field-aligned currents through the conductive layer at the base of the ionosphere, and the magnetic fields are produced directly by the currents. The basic geometry involved is illustrated in Figure 14. In this model, it can be shown that the electric and magnetic fields are related to the height-integrated Pedersen conductivity,  $B/(\mu_0 E) = \Sigma_p$ . Comparisons of the  $B/(\mu_0 E)$  ratio are in good agreement with estimates of the height-integrated Pedersen conductivity [Smiddy et al., 1980; Gurnett et al., 1984; Weimer et al., 1985]. The second model assumes that the noise is caused by Alfvén waves. Several investigators, for example, Goertz and Boswell [1979] and Lysak and Dum [1983], have pointed out that turbulent fluctuations imposed on the auroral field lines in the distant magnetosphere should be transmitted to the ionosphere as a shear Alfvén wave, or in a modified form called a kinetic Alfvén wave [Hasegawa, 1977]. Since large turbulent fluctuations are known to exist in the magnetopause boundary layer and in the distant magnetotail [Coroniti et al., 1977], there are good reasons to believe that large amplitude Alfvén waves should be excited along the auroral field lines. Chang et al. [1986] have suggested that these waves play an important role in auroral ion acceleration at low altitudes.

To decide between the static structure model and the Alfvén wave model, it is necessary to evaluate the Doppler shift caused by the spacecraft motion relative to the plasma. In the static structure model, the fluctuations are caused entirely by the Doppler shift, whereas in the Alfvén wave model, the Doppler shift is negligible.

An evaluation of the Doppler shift requires measurements of the wavelength, which can only be obtained from multi-spacecraft measurements. Unfortunately, such measurements do not exist so it is very difficult to determine which model provides the best description.

## ELECTROSTATIC WAVES

### Upper-Hybrid Waves and Electron Cyclotron Waves

As can be seen in Figure 2, there are two basic types of electrostatic waves that occur near the electron cyclotron frequency and plasma frequency. They are upper hybrid resonance waves and electron cyclotron waves. Although both types of waves are commonly found in other regions of the magnetosphere, particularly near the magnetic equatorial plane [Kennel et al., 1970; Shaw and Gurnett, 1975], they are seldom observed at high altitudes over the auroral zone. The absence of intense emissions at the upper-hybrid resonance frequency, and near harmonics of the electron cyclotron frequency is apparently related to the low plasma densities ( $f_{pe} \ll f_{ce}$ ) that usually occur at high altitudes over the auroral zone. When upper-hybrid and electron cyclotron waves are observed, they almost always occur when the electron density is high (i.e.,  $f_{pe} \gtrsim f_{ce}$ ). For example, an upper-hybrid noise band and a weak " $(3/2)f_{ce}$ " electron cyclotron emission can be seen in Figure 9 of Gurnett et al. [1983]. These events occur near the polar cusp on the dayside of the Earth under conditions where  $f_{pe} \sim f_{ce}$ . The electron density near the polar cusp is usually substantially higher than in the nightside auroral zone.

### Lower-Hybrid Waves

Early spacecraft VLF measurements showed that intense narrowband electrostatic emissions frequently occurred at the lower hybrid resonance frequency [Barrington, 1969]. Although these emissions are

a prominent feature of the plasma wave spectrum at middle and low latitudes, they are not normally observed in the auroral zone. Auroral hiss emissions are sometimes called "lower hybrid waves" [Chang and Coppi, 1981]. However, these emissions are actually electromagnetic whistler-mode waves, and have been described in the previous section.

### Electrostatic Ion Cyclotron Waves

In an early theoretical study of electrostatic instabilities, Kindel and Kennel [1971] predicted that electrostatic ion cyclotron waves should be generated at high altitudes over the auroral zones by field-aligned currents. Waves similar to those predicted by Kindel and Kennel were subsequently discovered by Kintner et al. [1978] using electric field measurements from the S3-3 satellite. Typically the electrostatic ion cyclotron waves appear as strong narrowband emissions at frequencies slightly above the proton cyclotron frequency and its harmonics. Kintner [1980] has distinguished between waves excited at low harmonic numbers,  $n \lesssim 3$ , which he called electrostatic ion cyclotron (EIC) waves, and waves excited at higher harmonic numbers, which he called ion cyclotron harmonic (ICH) waves. Both of these types of waves are illustrated in Figure 15. Typical electric field amplitudes are on the order of 1 mV/m [Koskinen et al., 1987], although field strengths of up to 25 mV/m have been reported in some cases [Kintner et al., 1978]. In both cases the electric field tends to be oriented nearly perpendicular to the static magnetic field. Phase velocity measurements by Kintner et al. [1984] and Doppler broadening analyses by Boardson et al. [1989]

show that the wavelengths are comparable to the proton cyclotron radius. Recently, electrostatic waves have also been discovered near harmonics of the oxygen cyclotron frequency [Kintner et al., 1988].

The free energy source that drives the electrostatic ion cyclotron waves and the possible role that these waves play in the physics of the auroral acceleration region is still somewhat uncertain. Comparisons with plasma distribution functions by Kintner et al. [1979], Kintner [1980], Cattell [1981], André [1986], and Koskinen et al. [1987] indicate that the electrostatic ion cyclotron mode can be driven unstable by ion beams and ion conic distributions as well as by field-aligned currents. The absence of adequate low energy electron measurements have made it difficult to evaluate the possible role of electrons as the free energy source. For several years it has been suggested [Lysak et al., 1980] that electrostatic ion cyclotron waves may play an important role in accelerating ion conic distributions. Although EIC and ICH waves are frequently observed in the region where the transverse ion heating occurs [Peterson et al., 1988], the role of these waves is uncertain. Generally, the intensities are quite low ( $\sim$  few mV/m). It is not clear that such low intensities can account for the observed heating rates.

#### Broadband Electrostatic Noise

For many years it has been known that intense broadband bursts of electrostatic noise occur along the auroral field lines. The first evidence of this noise was provided by Scarf et al. [1973, 1975] who identified impulsive bursts of electrostatic noise at

frequencies of 1 to 10 kHz over the nighttime auroral region in association with field-aligned currents. A similar type of noise was later found at lower frequencies in the distant magnetotail by Gurnett et al. [1976]. Subsequent studies by Gurnett and Frank [1977] showed that the noise extends over an essentially continuous region along the auroral field lines from altitudes of a few thousand km to as much as  $46 R_E$  in the distant magnetotail. Since the noise is electrostatic and has a very broad bandwidth, it is commonly referred to as "broadband electrostatic noise."

A representative spectrum of an intense broadband electrostatic noise event is shown in Figure 16. Typically, the noise extends over a very broad frequency range, from a few Hz to several tens of kHz, usually decreasing in intensity with increasing frequency. The integrated broadband electric field amplitude tends to decrease with increasing distance from the Earth, from about 10 to 30 mV/m at altitudes of a few thousand km, to 1 to 3 mV/m in the distant magnetotail. On a fine time scale the noise is very impulsive and spiky, and shows no simple relationship to any of the characteristic frequencies of the plasma. Recent studies by Erlandson et al. [1987] have shown that the impulsive variations are related to fine structure in the field-aligned current distribution. At low and intermediate altitudes, up to a few  $R_E$ , the broadband electrostatic noise tends to be imbedded in funnel-shaped auroral hiss events. For example, in Figure 7, the intense low frequency electric field noise from about 1232 to 1247 UT is broadband electrostatic noise. At high frequencies the broadband electrostatic noise is often difficult to distinguish from auroral hiss, and at low frequencies the noise

merges with the electric field component of the low frequency electric and magnetic noise described in the previous section. Isolated bursts of broadband electrostatic noise also sometimes occur over the polar cap, for example, from about 1157 to 1159 UT in Figure 7.

In addition to the correlation with field-aligned currents, comparisons with plasma measurements show that the broadband electrostatic noise is correlated with ion beams in the distant magnetotail [Grabbe and Eastman, 1984], and with ion conics at lower altitudes over the auroral zone [Chang et al., 1986]. Despite the association with energetic ions, the free energy responsible for the broadband electrostatic noise has still not been clearly established. In an early theory, Ashour-Abdalla and Thorne [1977] proposed that the noise is caused by electrostatic ion cyclotron waves driven by field-aligned currents. The high frequencies and absence of spectral structure at harmonics of the ion cyclotron frequency were thought to be due to Doppler spreading. More recently, Grabbe and Eastman [1984] proposed that the noise is produced by an electrostatic ion-beam instability. Their theory accounts for the broadband nature of the spectrum without the need to consider Doppler effects. A major difficulty in evaluating all of these interpretations is that the plasma wave mode has not been clearly established. In fact, the broadband nature of the noise and the complete absence of cutoffs or resonances at any of the characteristic frequencies of the plasma suggest that the usual small amplitude linearized mode analysis may not be applicable. Instead, the noise may represent a large amplitude turbulent state in which nonlinear effects play the dominant role. In this case, all evidence of the unstable plasma wave mode is effectively eliminated from the electric field spectrum.

## CONCLUSION

In this chapter we have reviewed the present state of understanding of auroral plasma waves. The observations are characterized by great diversity with many different plasma wave modes. At the present time, most of the primary wave phenomena associated with the aurora are known, and well-developed theories have been advanced to explain most of them. Although much progress has been made, many details yet remain to be resolved. For example, although the auroral kilometric radiation is widely believed to be generated by the cyclotron maser instability, the detailed feature of the electron distribution function that drives this instability still has not been firmly established. Similarly, the origin of the broadband electrostatic noise remains poorly understood, and the possible role of electrostatic ion cyclotron waves and Alfvén waves in the heating of auroral ion distributions has not been clearly established. It is clear from these and other similar issues that many detailed questions still remain unresolved. Most likely, the study of auroral plasma waves will continue to be an active area of research for many years to come.

## ACKNOWLEDGEMENTS

The author would like to thank A. Persoon, R. L. Huff, and R. R. Anderson for helping in the preparation of several of the illustrations, and L. A. Frank for providing the auroral image from Dynamics Explorer-1. This research was supported by NASA through Grants NAG5-310 and NAG5-1093 with Goddard Space Flight Center, and by Grant NAGW-1488 with NASA Headquarters.

## REFERENCES

- Alexander, J. K., and M. L. Kaiser, Terrestrial kilometric radiation.  
1. Spatial structure studies, J. Geophys. Res., 81, 5948-5956,  
1976.
- Andre, M., Electrostatic ion waves generated by ion loss-cone  
distributions in the magnetosphere, Annales Geophysicae, 4, 241-  
246, 1986.
- Armstrong, J. C., and A. J. Zmuda, Triaxial magnetic measurements of  
field-aligned currents at 800 km in the auroral region: Initial  
results, J. Geophys. Res., 78, 6802-6807, 1973.
- Ashour-Abdalla, M., and R. M. Thorne, The importance of electrostatic  
ion cyclotron instability for quiet-time auroral precipitation,  
Geophys. Res. Lett., 4, 45-48, 1977.
- Barrington, R. E., Satellite Observations of VLF Resonances, Plasma  
Waves in Space and Laboratory, Vol. 1, ed. by J. O. Thomas and B.  
J. Landmark, Edinburgh Press, Edinburgh, 361, 1969.
- Benediktov, E. A., G. G. Getmantsev, Yu. A. Sazonov, A. F. Tarasov,  
Preliminary results of measurements of the intensity of  
distributed extraterrestrial radio-frequency emission at 725 and  
1525-kHz frequencies by the satellite electron-2, Kosm. Issled.,  
3, 614-617, 1965.
- Benediktov, E. A., G. G. Getmantsev, N. A. Mityakov, V. O. Rapoport,  
and A. F. Tarasov, Relation between geomagnetic activity and the  
sporadic radio emission recorded by the elektron satellites, Kosm.  
Issled., 6, 946-949, 1968.

- Benson, R. F., M. M. Mellott, R. L. Huff, and D. A. Gurnett, Ordinary mode auroral kilometric radiation fine structure observed by DE-1, J. Geophys. Res., 93, 7515-7520, 1988.
- Boardsen, S., W. Peterson, and D. Gurnett, Double-peaked electrostatic ion cyclotron waves, J. Geophys. Res., submitted, 1989.
- Brown, L. W., The galactic radio spectrum between 130 kHz and 2600 kHz, Astrophys. J., 180, 359-370, 1973.
- Burke, B. F., and K. L. Franklin, Observations of a variable radio source associated with the planet Jupiter, J. Geophys. Res., 60, 213-217, 1955.
- Burton, E. T., and E. M. Boardman, Audio-frequency atmospheric, Proc. IRE, 21, 1476-1494, 1933.
- Carlqvist, P., and R. Bostrom, Space charge regions above the aurorae, J. Geophys. Res., 75, 7140-7146, 1970.
- Cattell, C., The relationship of field-aligned currents to electrostatic ion cyclotron waves, J. Geophys. Res., 86, 3641-3645, 1981.
- Chang, T., and B. Coppi, Lower hybrid acceleration and ion evolution in the supraauroral region, Geophys. Res. Lett., 8, 1253-1256, 1981.
- Chang, T., G. B. Crew, N. Hershkowitz, J. R. Jasperse, J. M. Retterer and J. D. Winningham, Transverse acceleration of oxygen ions by electromagnetic ion cyclotron resonance with broadband left-hand polarized waves, Geophys. Res. Lett., 13, 636-639, 1986.
- Coroniti, F. V., F. L. Scarf, L. A. Frank, and R. P. Lepping, Microstructure of a magnetotail fireball, Geophys. Res. Lett., 4, 219-222, 1977.

- Curtis, S. A., W. R. Hoegy, L. H. Brace, N. C. Maynard, and M. Sugiura, DE-2 cusp observations: Role of plasma instabilities in topside ionospheric heating and density fluctuations, Geophys. Res. Lett., 9, 997-1000, 1982.
- Dowden, R. L., Low frequency (100 kc/s) radio noise from the aurora, Nature, 184, 803, 1959.
- Duncan, R. A., and G. R. Ellis, Simultaneous occurrence of subvisual aurorae and radio noise bursts on 4.6 kc/s, Nature, 183, 1618-1619, 1959.
- Dunckel, N., B. Ficklin, L. Rorden, and R. A. Helliwell, Low frequency noise observed in the distant magnetosphere with OGO 1, J. Geophys. Res., 75, 1854-1862, 1970.
- Ellis, G. R., Low-frequency radio emission auroral, J. Atmos. Terrestr. Phys., 10, 302-306, 1957.
- Erlandson, R. E., R. Pottetelette, T. A. Potemra, L. J. Zanetti, A. Bahnsen, R. Lundin, and M. Hamelin, Impulsive electrostatic waves and field-aligned currents observed in the entry layer, Geophys. Res. Lett., 14, 431-434, 1987.
- Frank, L. A., and K. L. Ackerson, Observations of charged-particle precipitation into the auroral zone, J. Geophys. Res., 76, 3612-3643, 1971.
- Gallagher, D. L., and D. A. Gurnett, Auroral kilometric radiation: Time-averaged source position, J. Geophys. Res., 84, 6501-6509, 1979.
- Gary, S. P., Electrostatic instabilities in plasmas with two components, J. Geophys. Res., 90, 8213-8221, 1985.

- Goertz, C. K., and R. W. Boswell, Magnetosphere-ionosphere coupling, J. Geophys. Res., 84, 7239-7246, 1979.
- Grabbe, C. L., Auroral kilometric radiation: A theoretical review, Rev. Geophys. and Space Phys., 19, 627-633, 1981.
- Grabbe, C. L., and T. E. Eastman, Generation of broadband electrostatic noise by ion beam instabilities in the magnetotail, J. Geophys. Res., 89, 3865-3872, 1984.
- Gregory, P. C., Radio emission from auroral electrons, Nature, 221, 350-352, 1969.
- Gurnett, D. A., A satellite study of VLF hiss, J. Geophys. Res., 71, 5599-5615, 1966.
- Gurnett, D. A., The Earth as a radio source: Terrestrial kilometric radiation, J. Geophys. Res., 79, 4227-4238, 1974.
- Gurnett, D. A., R. R. Anderson, F. L. Scarf, R. W. Fredricks, and E. J. Smith, Initial results from the ISEE-1 and -2 plasma wave investigation, Space Sci. Rev., 23, 103-122, 1979.
- Gurnett, D. A., and L. A. Frank, ELF noise bands associated with auroral electron precipitation, J. Geophys. Res., 77, 3411-3417, 1972.
- Gurnett, D. A., and L. A. Frank, A region of intense plasma wave turbulence on auroral field lines, J. Geophys. Res., 82, 1031-1050, 1977.
- Gurnett, D. A., L. A. Frank and R. P. Lepping, Plasma waves in the distant magnetotail, J. Geophys. Res., 81, 6059-6071, 1976.

- Gurnett, D. A., R. L. Huff, J. D. Menietti, J. L. Burch, J. D. Winningham, and S. D. Shawhan, Correlated low-frequency electric and magnetic noise along the auroral field lines, J. Geophys. Res., 89, 8971-8985, 1984.
- Gurnett, D. A., and B. J. O'Brien, High-Latitude geophysical studies with Satellite Injun 3. 5. Very-low-frequency electromagnetic radiation, J. Geophys. Res., 69, 65-89, 1964.
- Gurnett, D. A., S. D. Shawhan, and R. R. Shaw, Auroral hiss, Z-mode radiation, and auroral kilometric radiation in the polar magnetosphere: DE 1 observations, J. Geophys. Res., 88, 329-340, 1983.
- Harang, L., and R. Larsen, Radio wave emissions in the VLF band observed near the auroral zone. 1. Occurrence of emissions during disturbances, J. Atmosph. Terr. Phys., 27, 481-497, 1964.
- Hartz, T. R., Low frequency noise emissions and their significance for energetic particle processes in the polar ionosphere, in The Polar Ionosphere and Magnetospheric Processes, ed. by G. Skovli, Gordon and Breach, New York, p. 151-160, 1970.
- Hashimoto, K., W. Calvert, and R. Huff, On Z-mode waves observed by the DE-1 satellite, Solar Terrestrial Environment Workshop, Tokyo, Japan, January 22, 1987.
- Hasegawa, A., Kinetic properties of Alfvén waves, Proc. Indian Acad. Sci., 86, 151, 1977.
- Helliwell, R. A., Whistlers and Related Ionospheric Phenomena, Stanford University Press, Stanford, CA, 1965.

- Heppner, J. P., Magnetospheric convection patterns inferred from high latitude activity, Atmospheric Emissions, ed. by B. M. McCormac and A. Omholt, Reinhold, N. York, 251, 1969.
- Huff, R. L., W. Calvert, J. D. Craven, L. A. Frank, and D. A. Gurnett, Mapping of auroral kilometric radiation sources to the aurora, J. Geophys. Res., 93, 11,445-11,454, 1988.
- James, H. G., VLF saucers, J. Geophys. Res., 81, 501-514, 1976.
- Jorgensen, T. S., and E. Ungstrup, Direct observation of correlation between aurorae and hiss in Greenland, Nature, 194, 462-463, 1962.
- Kelley, M. C., and P. Kintner, Two-dimensional turbulence in a low b cosmic scale plasma, Astrophys. J., 220, 339-345, 1978.
- Kelley, M. C., and F. S. Mozer, A satellite survey of vector electric fields in the ionosphere at frequencies of 10 to 500 Hz, 1, Isotropic, high-latitude electrostatic emissions, J. Geophys. Res., 77, 4158, 1972.
- Kennel, C. F., F. L. Scarf, R. W. Fredricks, J. H. McGehee, and F. V. Coroniti, VLF electric field observations in the magnetosphere, J. Geophys. Res., 75, 6136-6152, 1970.
- Kindel, J. M., and C. F. Kennel, Topside current instabilities, J. Geophys. Res., 76, 3055-3078, 1971.
- Kintner, P. M., Jr., Observations of velocity shear driven plasma turbulence, J. Geophys. Res., 81, 5114-5122, 1976.
- Kintner, P. M., On the distinction between electrostatic ion cyclotron waves and ion cyclotron harmonic waves, Geophys. Res. Lett., 7, 585-588, 1980.

- Kintner, P. M., M. C. Kelley, and F. S. Mozer, Electrostatic hydrogen cyclotron waves near one earth radius altitude in the polar magnetosphere, Geophys. Res. Lett., 5, 139-142, 1978.
- Kintner, P. M., M. C. Kelley, R. D. Sharp, A. G. Ghielmetti, M. Temerin, C. Cattell, P. F. Mizera, and J. F. Fennell, Simultaneous observations of energetic (keV) upstreaming and electrostatic hydrogen waves, J. Geophys. Res., 84, 7201-7212, 1979.
- Kintner, P. M., J. LaBelle, M. C. Kelley, L. J. Cahill, Jr., T. Moore, and R. Arnoldy, Interferometric phase velocity measurements, Geophys. Res. Lett., 11, 19-22, 1984.
- Kintner, P. M., J. Vago, R. Arnoldy, and T. Moore, Simultaneous observations of electrostatic oxygen cyclotron waves and ion conics, EOS Trans. Am. Geophys. Union, 69, 1396, 1988.
- Koskinen, H. E. J., P. M. Kintner, G. Holmgren, B. Holback, G. Gustafsson, M. Andre, and R. Lundin, Observations of ion cyclotron harmonic waves by the Viking satellite, Geophys. Res. Lett., 14, 459-462, 1987.
- Krall, N. A., and A. W. Trivelpiece, Principles of Plasma Physics, McGraw-Hill, N. York, 1973.
- Kurth, W. S., M. M. Baumbach, and D. A. Gurnett, Direction-finding measurements of auroral kilometric radiation, J. Geophys. Res., 80, 2764-2770, 1975.
- Laaspere, T., and R. A. Hoffman, New results on the correlaton between low-energy electrons and auroral hiss, J. Geophys. Res., 81, 524-530, 1976.

- Lin, C. S., J. L. Burch, S. D. Shawhan and D. A. Gurnett, Correlation of auroral hiss and upward electron beams near the polar cusp, J. Geophys. Res., 89, 925-935, 1984.
- Louarn, P., A. Roux, H. deFeraudy, and D. LeQueau, Trapped electrons as a free energy source for the AKR, J. Geophys. Res., submitted, 1989.
- Lysak, R. L., and C. T. Dum, Dynamics of magnetosphere-ionosphere coupling including turbulent transport, J. Geophys. Res., 88, 365-380, 1983.
- Lysak, R. L., M. K. Hudson, and M. Temerin, Ion heating by strong electrostatic ion cyclotron heating, J. Geophys. Res., 85, 678-686, 1980.
- Maggs, J. E., Coherent generation of VLF hiss, J. Geophys. Res., 81, 1707-1724, 1976.
- Maggs, J. E., and W. Lotko, Altitude dependent model of the auroral beam and beam-generated electrostatic noise, J. Geophys. Res., 86, 3439-3447, 1981.
- Martin, L. H., R. A. Helliwell, and K. R. Marks, Association between aurorae and very-low-frequency hiss observed by Byrd Station, Antarctica, Nature, 187, 751-753, 1960.
- Maynard, N. C., and J. P. Heppner, Variations in electric fields from polar orbiting satellites, Particles and Fields in the Magnetosphere, ed. by B. M. McCormac, Reinhold, N. York, 247-253, 1970.

- Mellott, M. M., W. Calvert, R. L. Huff, D. A. Gurnett and S. D. Shawhan, DE-1 observations of ordinary mode and extraordinary mode auroral kilometric radiation, Geophys. Res. Lett., 11, 1188-1191, 1984.
- Melrose, D. B., Coherent gyromagnetic emission as a radiation mechanism, Aust. J. Phys., 26, 229, 1973.
- Morioka, A., H. Oya, and S. Miyatake, Terrestrial kilometric radiation observed by satellite JIKIKEN (EXOS-B), J. Geomag. Geoelectr., 33, 37-62, 1981.
- Morozumi, H. M., Semi-diurnal auroral peak and VLF emissions observed at the south pole, 1960, EOS Trans. Am. Geophys. Union, 44, 798, 1963.
- Mosier, S. R., and D. A. Gurnett, VLF measurements of the Poynting flux along the geomagnetic field with the Injun 5 satellite, J. Geophys. Res., 74, 5675-5687, 1969.
- Mosier, S. R., M. L. Kaiser, and L. W. Brown, Observations of noise bands associated with the upper hybrid resonance by the IMP 6 radio astronomy experiment, J. Geophys. Res., 78, 1683, 1973.
- Omidi, N., and D. A. Gurnett, Growth rate calculations of auroral kilometric radiation using the relativistic resonance condition, J. Geophys. Res., 87, 2377-2383, 1982.
- Omidi, N., C. S. Wu, and D. A. Gurnett, Generation of auroral kilometric and Z mode radiation by the cyclotron maser mechanism, J. Geophys. Res., 89, 883-895, 1984.
- Persoon, A. M., and D. A. Gurnett, The high-resolution frequency spectrum of Z mode radiation, EOS Trans. AGU, 70, 434, 1989.

- Peterson, W. K., E. G. Shelley, S. A. Boardsen, D. A. Gurnett, B. G. Ledley, M. Sugiura, T. E. Moore, and J. H. Waite, Transverse ion energization and low-frequency plasma waves in the mid-altitude auroral zone: A case study, J. Geophys. Res., 93, 11,405-11,428, 1988.
- Ratcliffe, J. A., The Magneto-Ionic Theory and Its Applications to the Ionosphere, Cambridge University Press, N. York, 1959.
- Scarf, F. L., R. W. Fredricks, C. T. Russell, M. Kivelson, M. Neugebauer, and C. R. Chappell, Observation of a current-driven plasma instability at the outer zone-plasma sheet boundary, J. Geophys. Res., 78, 2150-2165, 1973.
- Scarf, F. L., R. W. Fredricks, C. T. Russell, M. Neugebauer, M. Kivelson, and C. R. Chappell, Current-driven plasma instabilities at high latitudes, J. Geophys. Res., 80, 2030-2040, 1975.
- Shaw, R. R., and D. A. Gurnett, Electrostatic noise bands associated with the electron gyrofrequency and plasma frequency in the outer magnetosphere, J. Geophys. Res., 80, 4259-4271, 1975.
- Shawhan, S. D., and D. A. Gurnett, Polarization measurements of auroral kilometric radiation by Dynamics Explorer-1, Geophys. Res. Lett., 9, 913-916, 1982.
- Smiddy, M., W. J. Burke, M. C. Kelley, N. A. Saflekos, M. S. Gussenhoven, D. A. Hardy, and F. J. Rich, Effects of high-altitude conductivity on observed convection electric fields and Birkeland currents, J. Geophys. Res., 85, 6811-6818, 1980.
- Smith, R. L., and N. Brice, Propagation in multicomponent plasmas, J. Geophys. Res., 69, 5029-5040, 1964.

- Stix, T. H., The Theory of Plasma Waves, McGraw-Hill, N. York, 1962.
- Stone, R. G., Radio physics of the outer solar system, Space Sci. Rev., 14, 534-551, 1973.
- Storey, L. R. O., An investigation of whistling atmospherics, Phil. Trans. Roy. Soc. London, A, 246, 113-141, 1953.
- Temerin, M., The polarization, frequency, and wavelength of high latitude turbulence, J. Geophys. Res., 83, 2609-2616, 1978.
- Temerin, M., and R. L. Lysak, Electromagnetic ion cyclotron mode (ELF) waves generated by auroral electron precipitation, J. Geophys. Res., 89, 2849-2859, 1984.
- Tokar, R. L., and S. P. Gary, Electrostatic hiss and the beam driven electron acoustic instability in the dayside polar cusp, Geophys. Res. Lett., 11, 1180-1183, 1984.
- Voots, G. R., D. A. Gurnett, and S.-I. Akasofu, Auroral kilometric radiation as an indicator of auroral magnetic disturbances, J. Geophys. Res., 82, 2259-2266, 1977.
- Walsh, D., T. F. Haddock, and H. F. Schulte, Cosmic radio intensities at 1.225 and 2.0 MC measured up to an altitude of 1700 km, Space Res., 4, 935, 1964.
- Weimer, D. R., C. K. Goertz, D. A. Gurnett, N. C. Maynard, J. L. Burch, Auroral zone electric fields from DE 1 and 2 at magnetic conjunctions, J. Geophys. Res., 90, 7479-7494, 1985.
- Winglee, R. M., Effects of a finite plasma temperature on electron-cyclotron maser emission, Astrophys. J., 291, 160-169, 1985.
- Wu, C. S., and L. C. Lee, A theory of terrestrial kilometric radiation, Astrophys. J., 230, 621-626, 1979.

Wu, C. S., S. T. Tsai, M. J. Xu, and J. W. Shen, Saturation and energy conversion efficiency of auroral kilometric radiation, Astrophys. J., 248, 384-391, 1981.

Zarka, P., D. LeQueau, and F. Genova, The maser synchrotron instability in an inhomogeneous medium: Determination of the spectral intensity of auroral kilometric radiation, J. Geophys. Res., 91, 13,542-13,558, 1986.

## FIGURE CAPTIONS

- Figure 1            The frequency range of the six most important electromagnetic modes and their relationship to various characteristic frequencies. The plasma parameters used to make these plots are representative of the auroral ionosphere.
- Figure 2            The characteristic frequencies of the various electrostatic modes that can exist along the auroral field lines.
- Figure 3            A frequency-time spectrogram of auroral kilometric radiation. This radio emission usually occurs in the frequency range from 100 to 400 kHz and is highly variable, both in frequency and amplitude.
- Figure 4            Representative ray paths for the auroral kilometric radiation. The propagation cutoff surface prevents the radiation from reaching the ground. This cutoff is at  $f_{R=0}$  for the R-X mode, and at  $f_{pe}$  for the L-O mode.
- Figure 5            A spectrogram showing the polarization of the auroral kilometric radiation. The dominant polarization is right-hand with respect to the magnetic field in the source region (R-X mode). A weak left-hand component is also sometimes observed (L-O mode).

- Figure 6 An auroral image from DE-1 showing the occurrence of bright auroral emissions during an intense AKR event. The dashed lines show the magnetic field lines through the source. The source position is determined from the intersection of the direction of arrival and the  $f = f_{ce}$  surface.
- Figure 7 A spectrogram of auroral hiss and Z-mode radiation during a DE-1 pass over the auroral zone.
- Figure 8 A spectrum showing the auroral hiss cutoff at  $f_{pe}$ , and the weaker Z-mode radiation above the cutoff. The frequency ranges of the four high frequency electromagnetic modes are given at the top of the plot.
- Figure 9 Representative ray paths of auroral hiss. Both upgoing and downgoing auroral hiss are observed. The upgoing auroral hiss has an upper frequency limit of  $f_{pe}$  or  $f_{ce}$ , whichever is smaller.
- Figure 10 Representative ray paths of Z-mode radiation. This radiation is trapped between the propagation cutoffs at  $f_{UHR}$  and  $f_{L=0}$ , and can propagate long distances over the polar cap.
- Figure 11 A frequency-time spectrogram of an ELF noise band observed over the auroral zone in association with an inverted-V electron precipitation event.
- Figure 12 ELF noise bands are believed to be caused by electromagnetic ion cyclotron waves propagating at large wave normal angles between the  $He^+$  and  $H^+$

cyclotron frequencies. These waves undergo a polarization reversal at the crossover frequency,  $f_x$ , and are reflected slightly below the ion hybrid resonance,  $f_{IHR}$ .

Figure 13 Representative spectrums of the low-frequency electric and magnetic field noise commonly observed at low altitudes over the auroral zone. The electric and magnetic fields are highly correlated at low frequencies, with the Poynting flux directed downward toward the Earth.

Figure 14 The low frequency electric and magnetic field noise is believed to be caused by the motion of the spacecraft through a system of quasi-static fields generated by field-aligned currents closing through the base of the ionosphere.

Figure 15 A frequency-time spectrogram of electrostatic ion-cyclotron waves detected by the S3-3 satellite. Two types have been identified: electrostatic hydrogen cyclotron waves (EHC), which occur at low harmonic numbers ( $n \leq 3$ ), and ion cyclotron harmonics (ICH), which occur at high harmonic numbers.

Figure 16 A spectrum of broadband electrostatic noise detected by the ISEE-1 spacecraft at high altitudes over the auroral zone. This noise is electrostatic and extends over a very broad frequency range, typically from a few Hz to more than ten kHz.

ELECTROMAGNETIC MODES

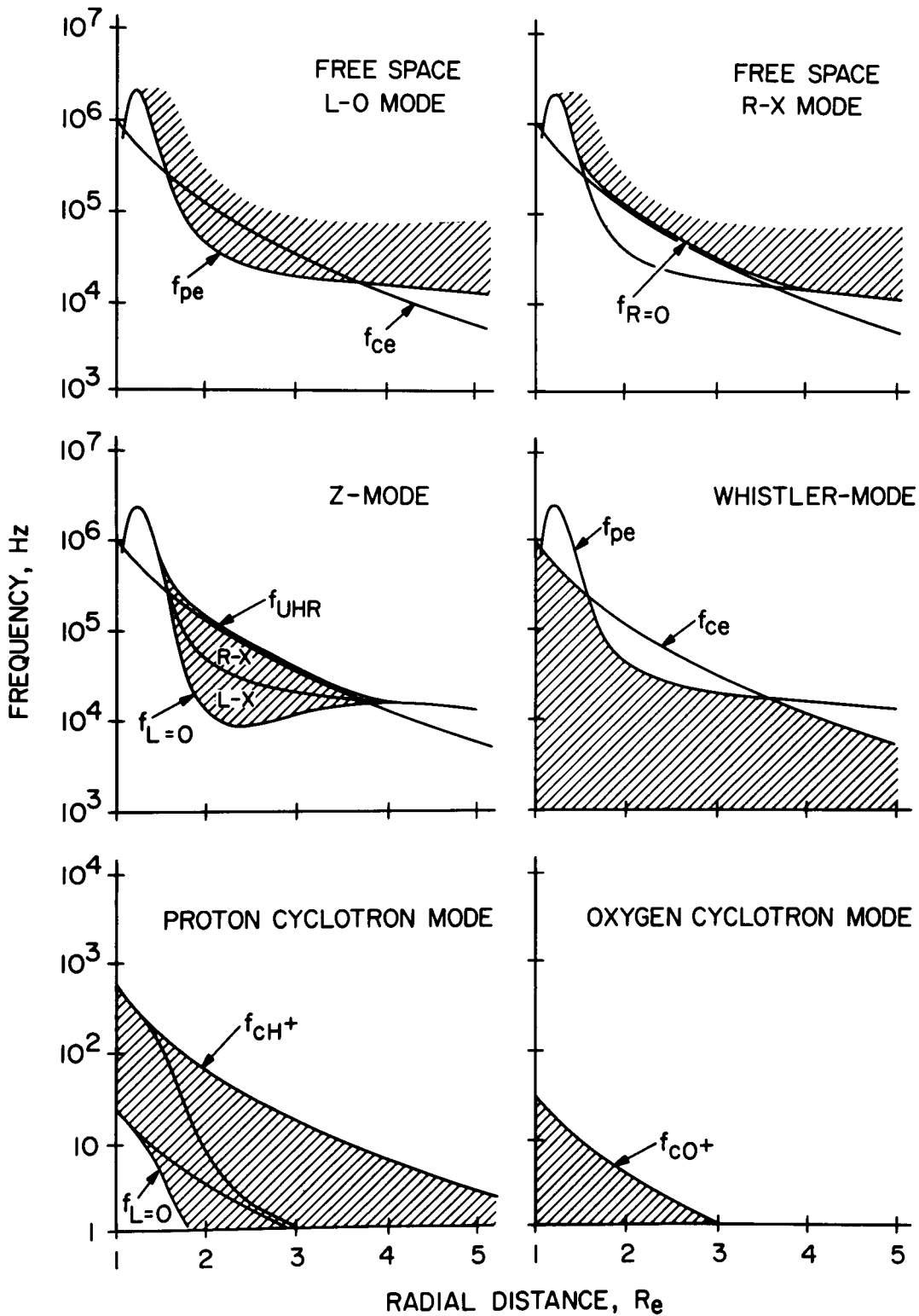


Figure 1

A-G89-77-2

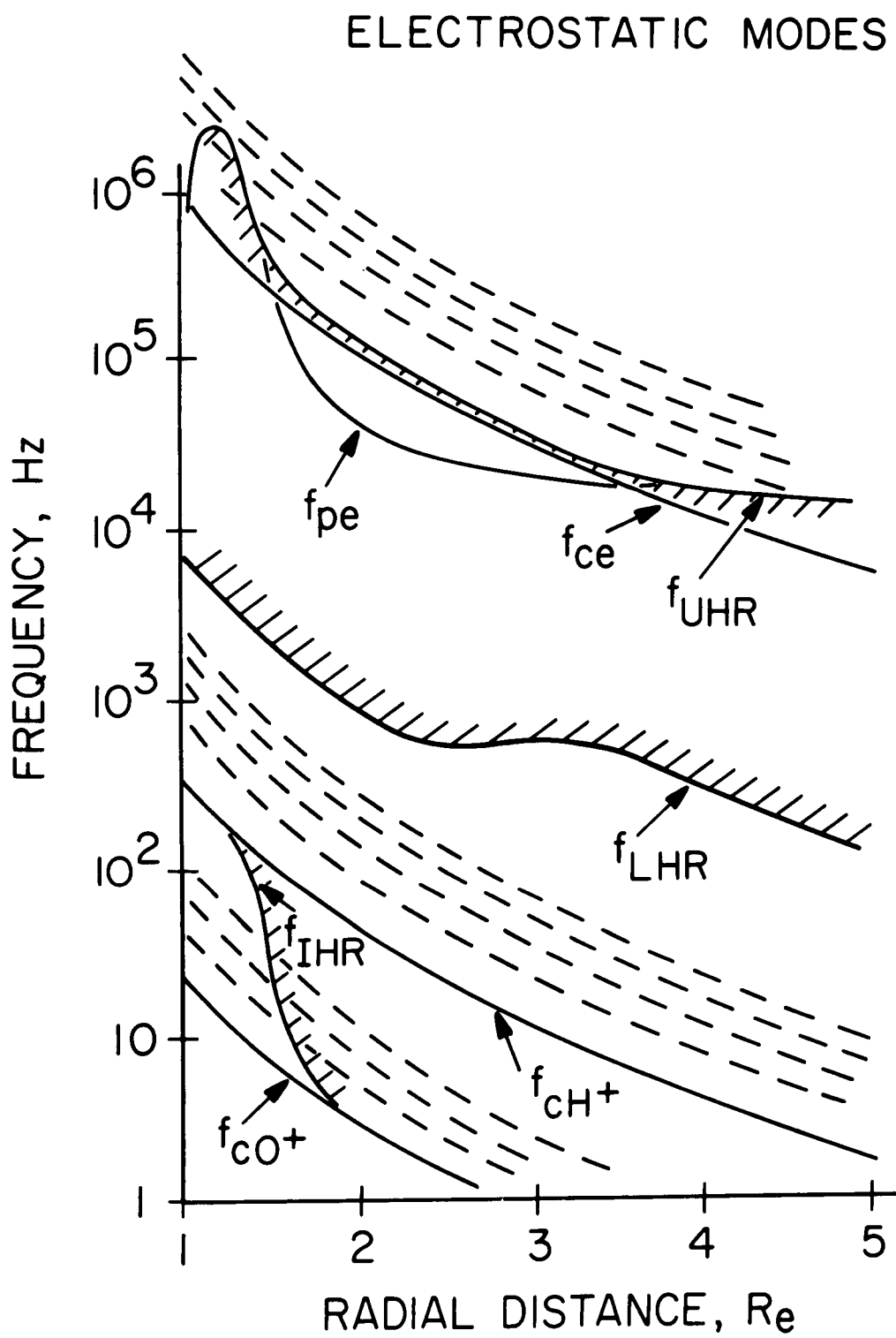
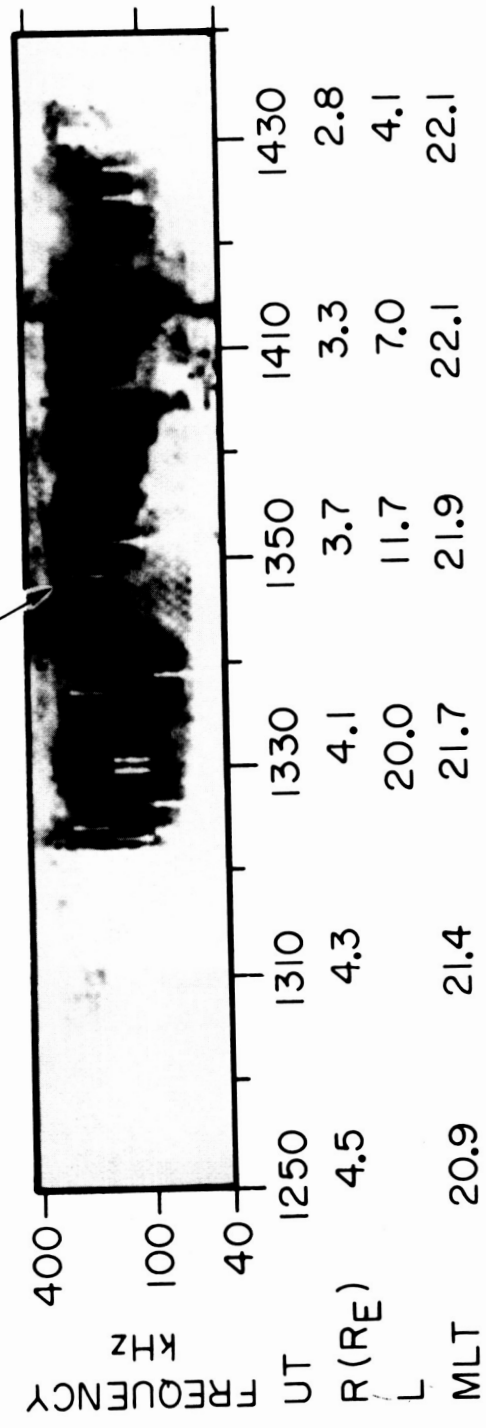


Figure 2

A-G82-229-1

AURORAL KILOMETRIC RADIATION



DE-1, OCTOBER 2, 1981

ORIGINAL PAGE  
BLACK AND WHITE PHOTOGRAPH

Figure 3

A-G74-51-3

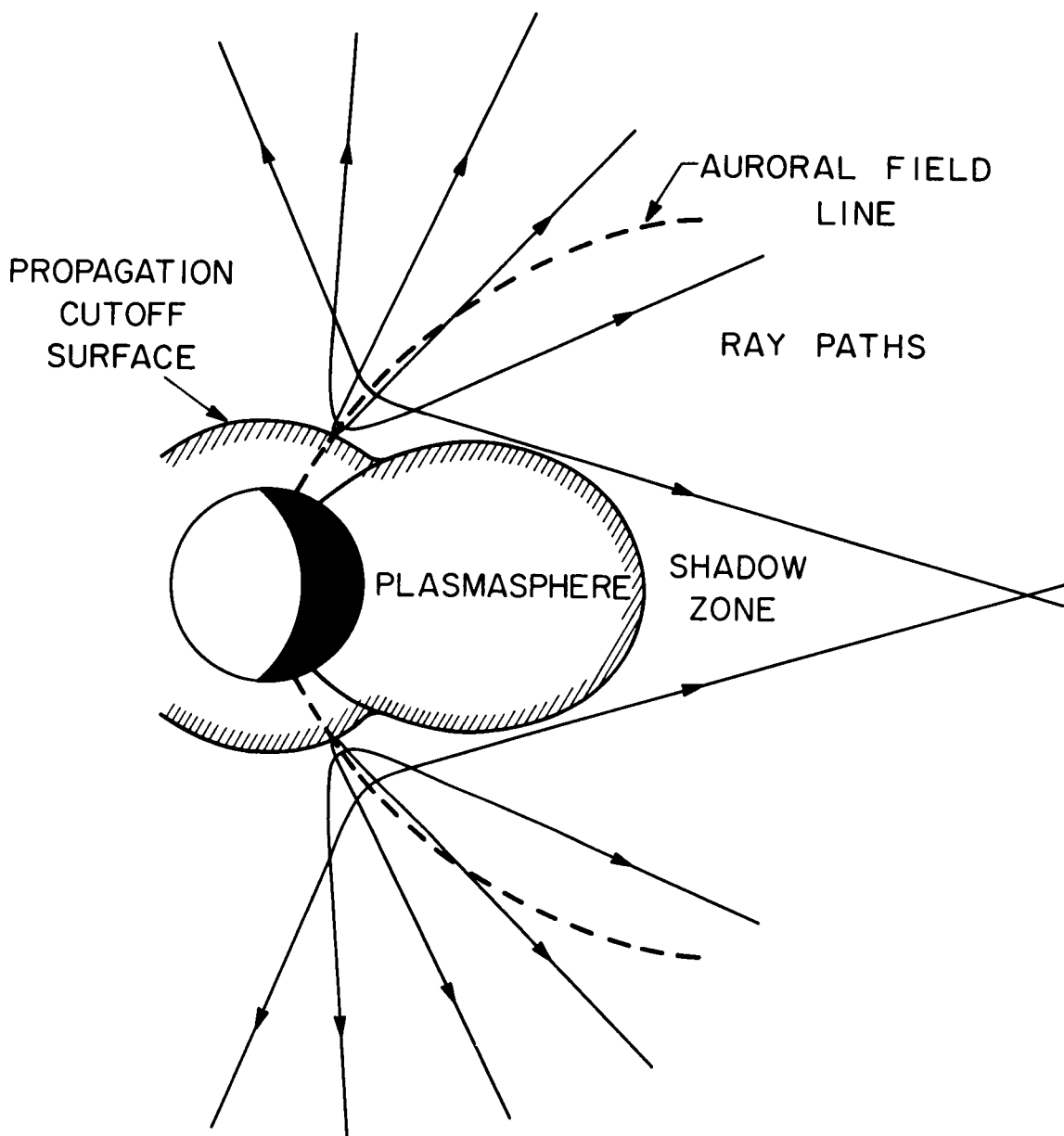


Figure 4

A-689-87

DE-1 PWI NOVEMBER 19, 1981 ORBIT 380

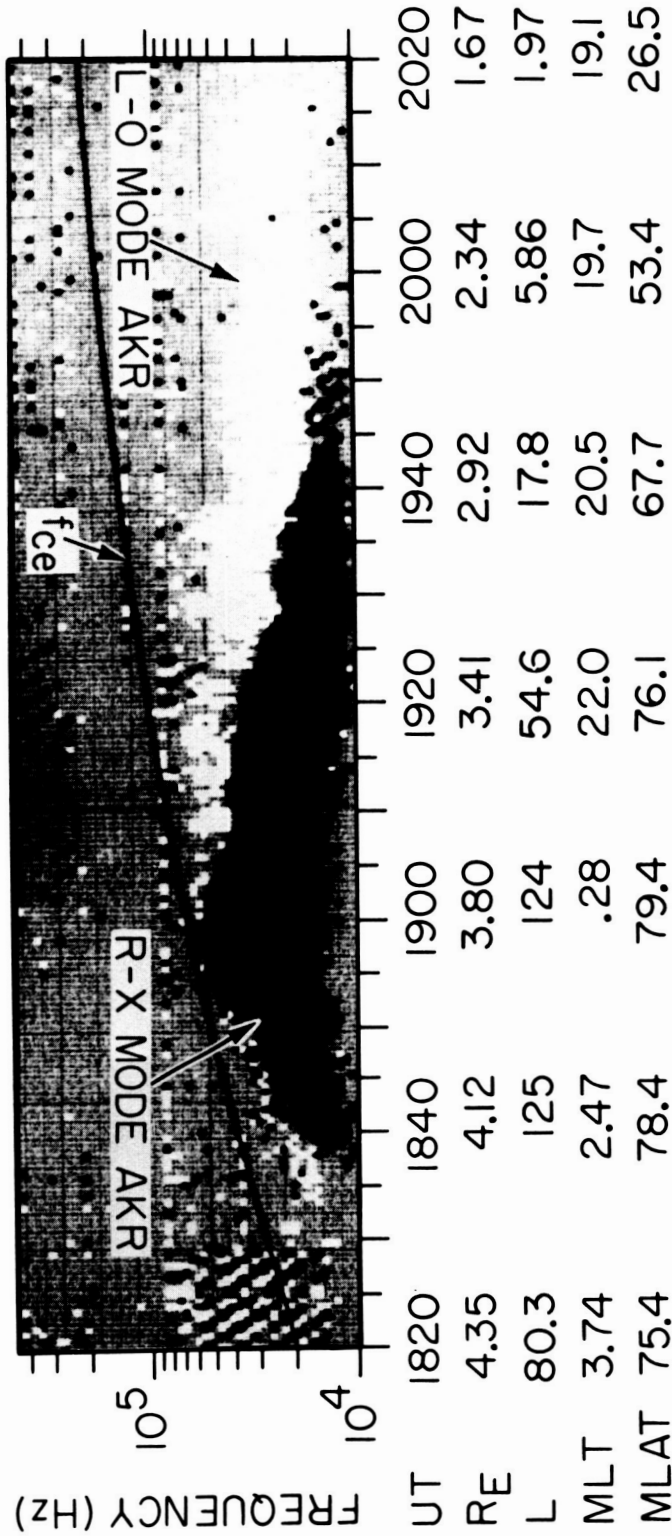


Figure 5

DE-1    JANUARY 27,    DAY 27,    1982    0445 UT



AKR SOURCE #	PWI		WAVE FREQUENCY
	UT		
1	0445		104 KHZ
2	0445		136 KHZ
3	0445		170 KHZ
4	0445		218 KHZ

ORIGINAL PAGE  
BLACK AND WHITE PHOTOGRAPH

Figure 6

A-G89-86

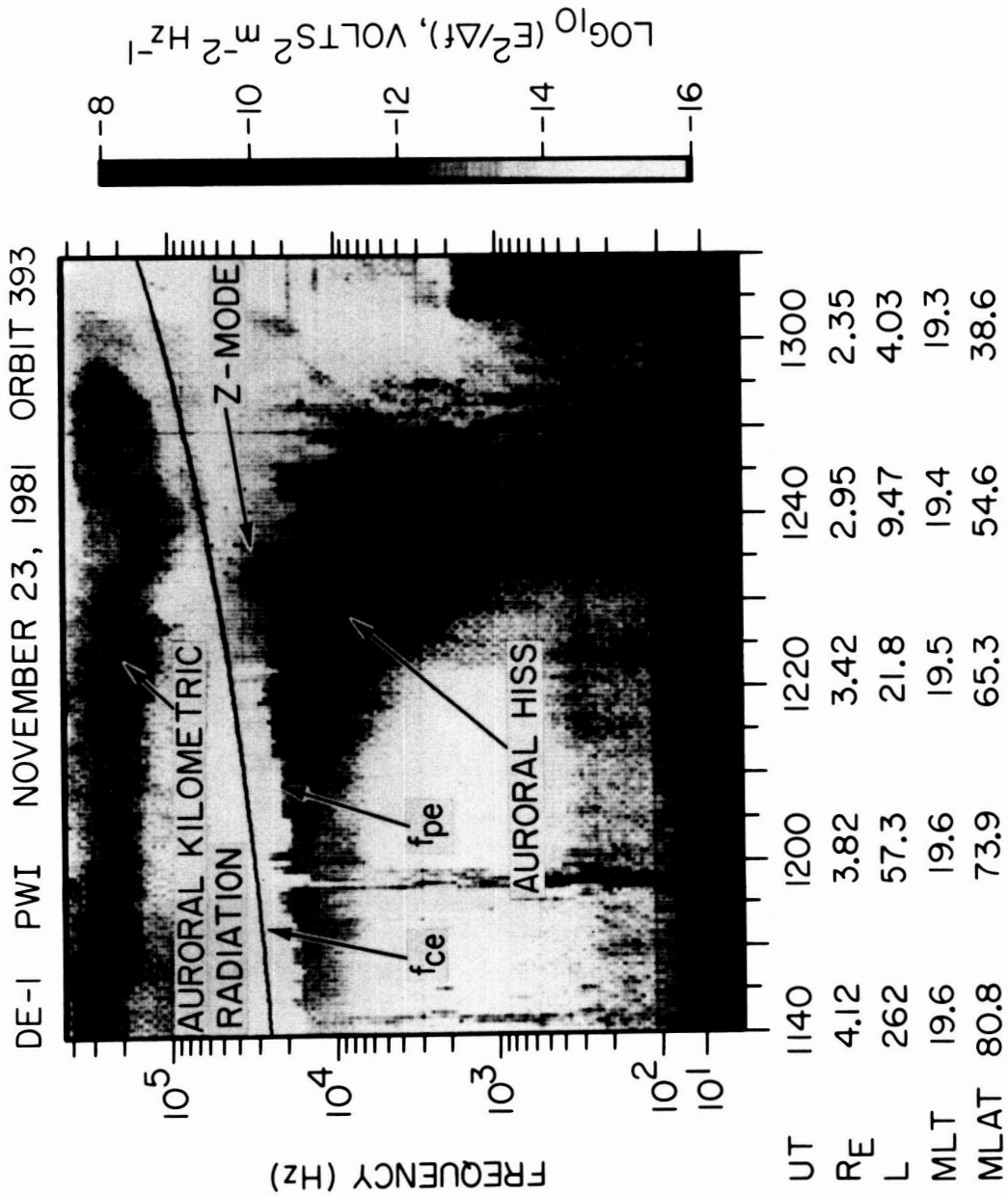


Figure 7

ORIGINAL PAGE  
 BLACK AND WHITE PHOTOGRAPH

C-G89-134

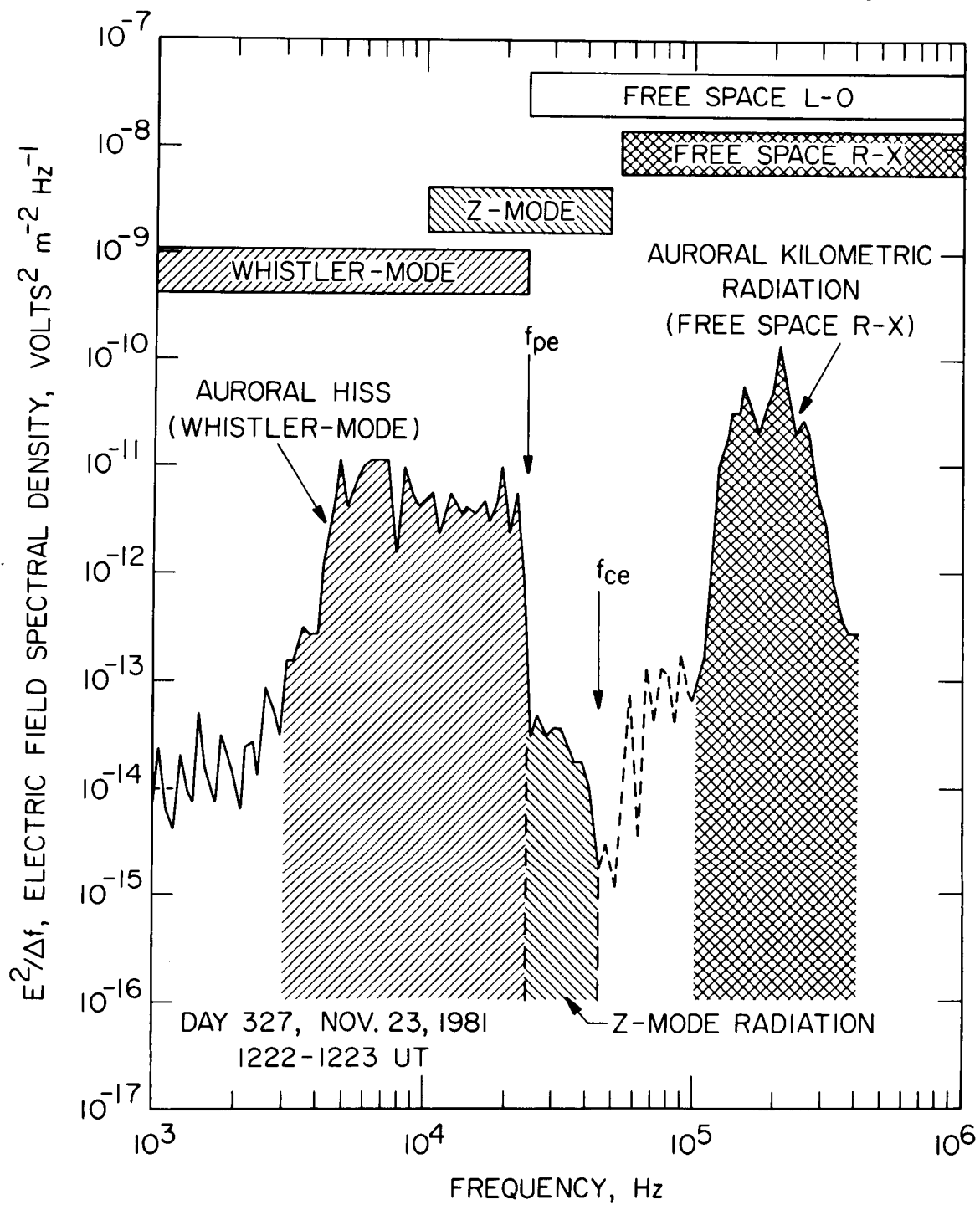


Figure 8

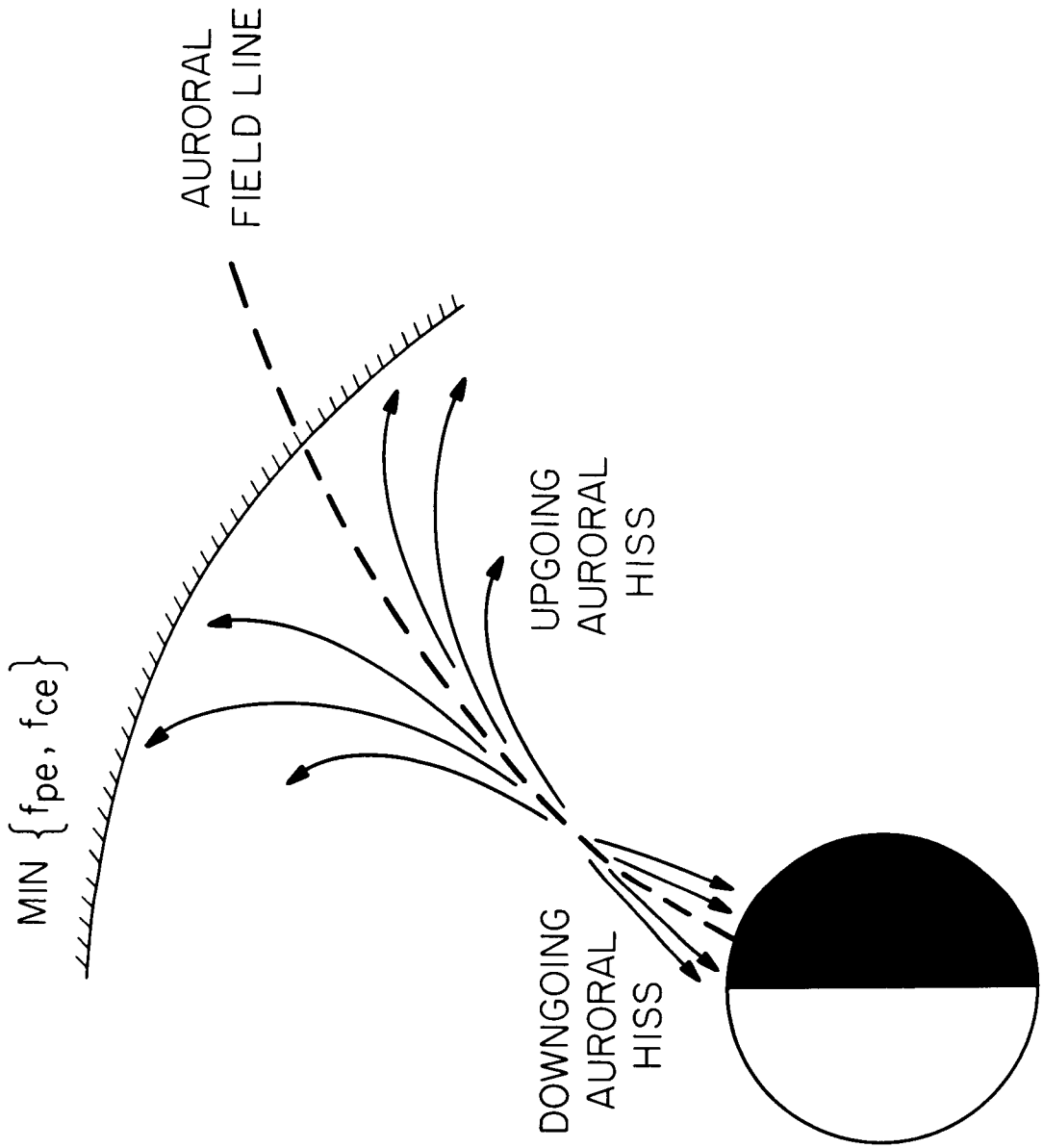


Figure 9

A-689-167

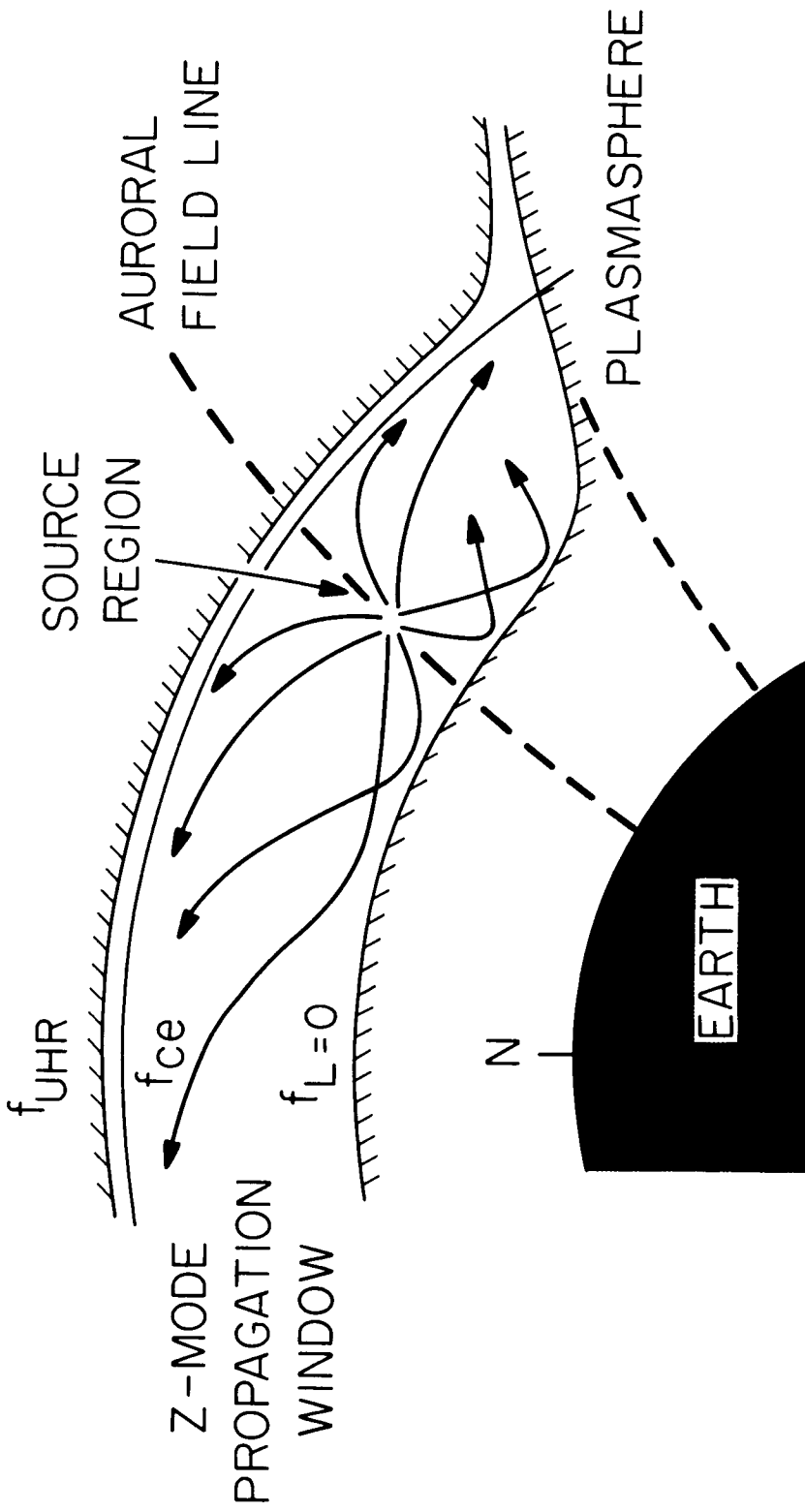
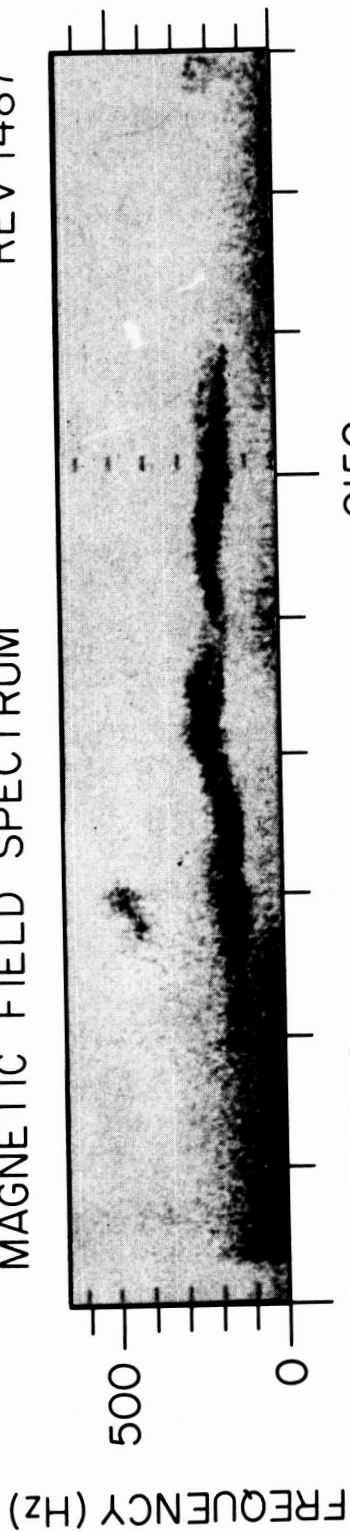


Figure 10

A-G89-183

REV 1487

MAGNETIC FIELD SPECTRUM



0150

68.5

61.5

UT: 0149 (HR MIN)

INV: 70.4°

MLT: 21.4 (HR)

INJUN 5, DECEMBER 9, 1968

ORIGINAL PAGE IS  
OF POOR QUALITY

Figure 11

B-G89-187-1

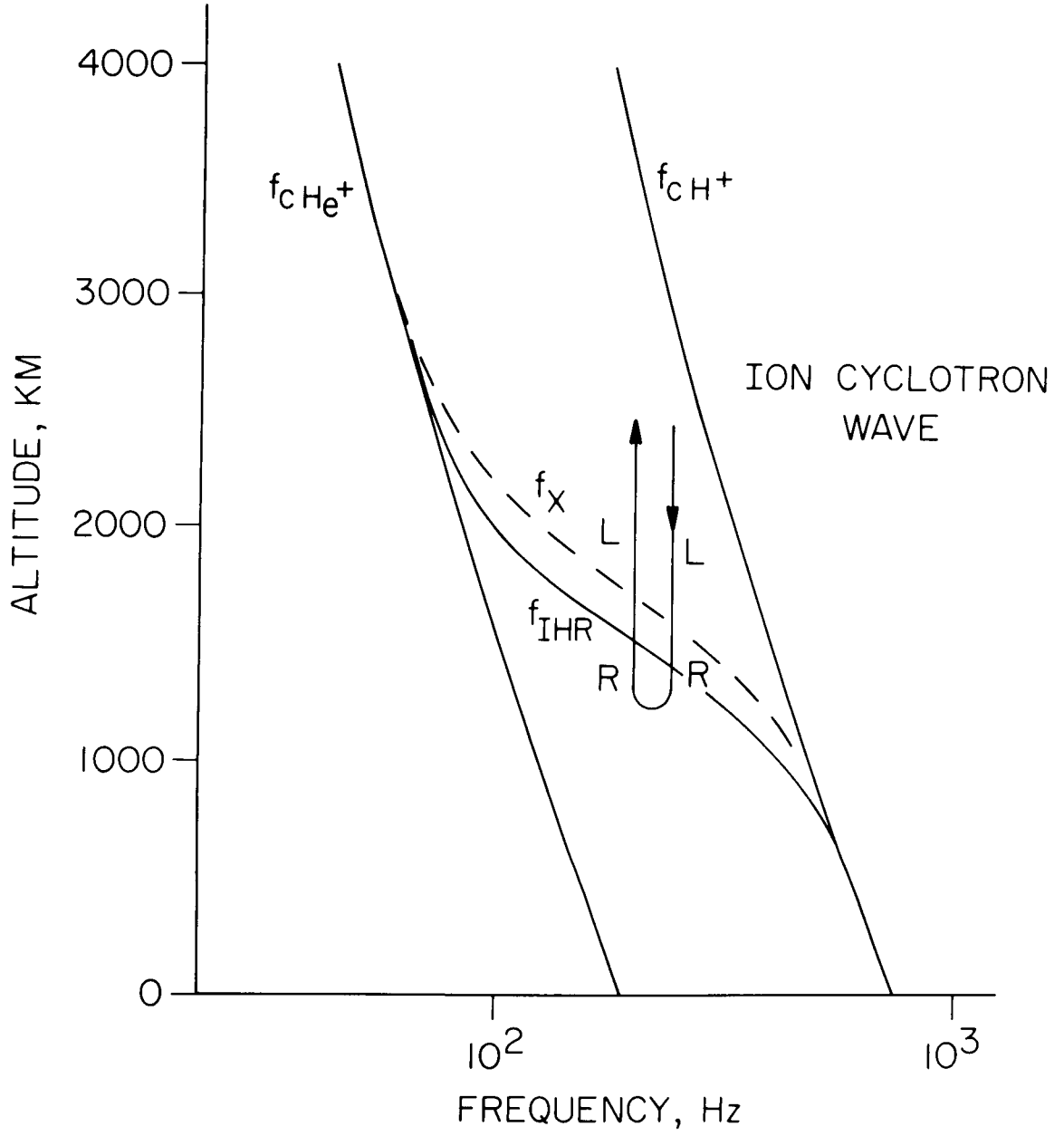


Figure 12

A-G89-189

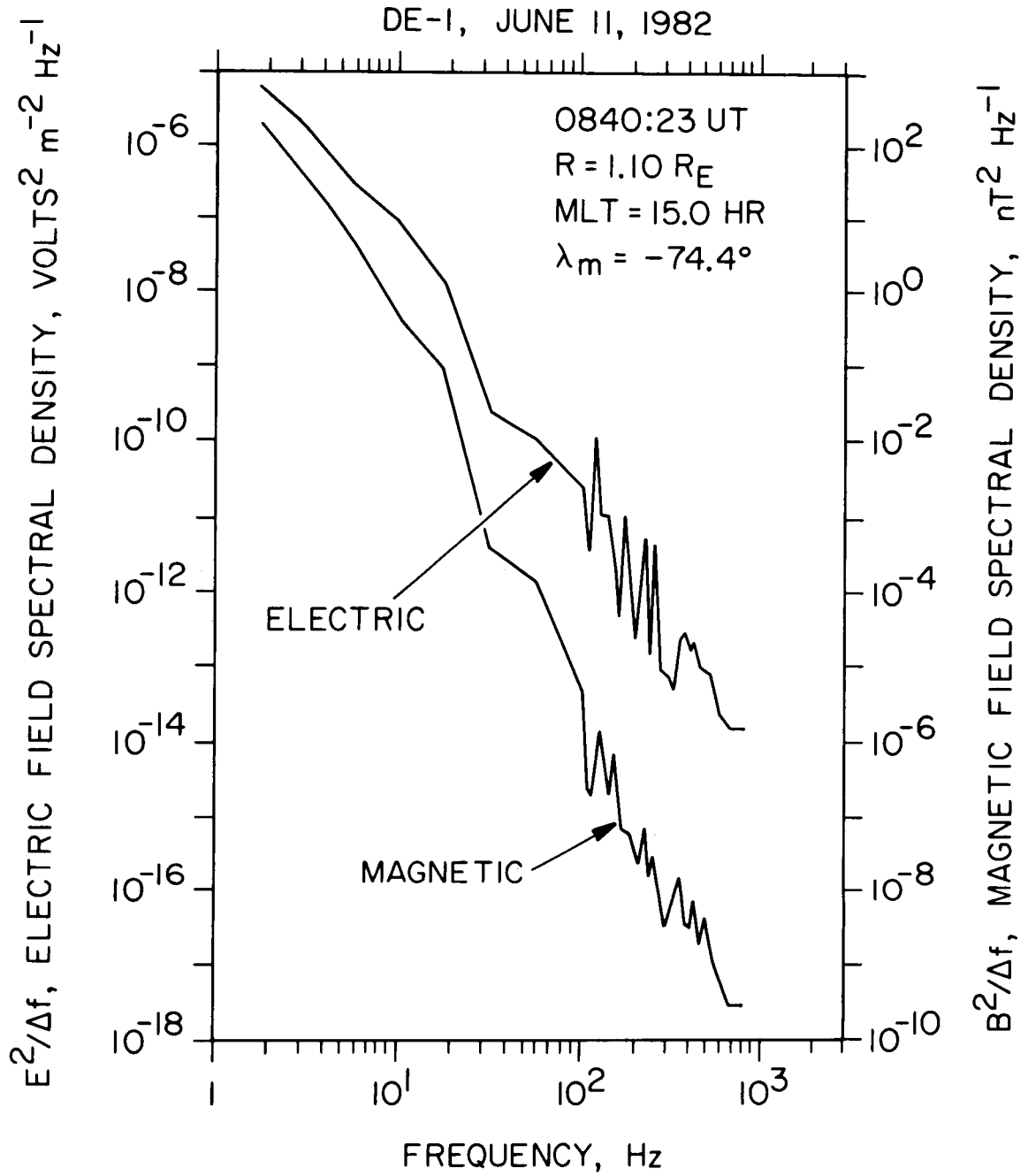
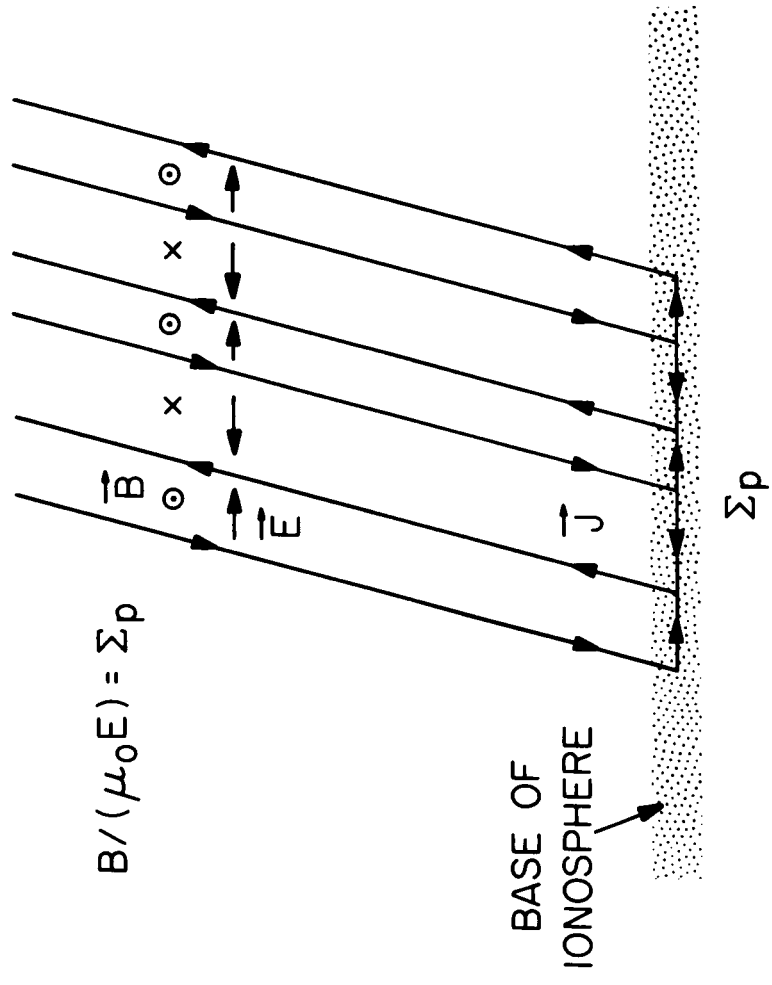


Figure 13

FIELD-ALIGNED CURRENTS



$$B / (\mu_0 E) = \Sigma p$$

Figure 14

S3-3 ELECTRIC FIELD 5/6 REV 757

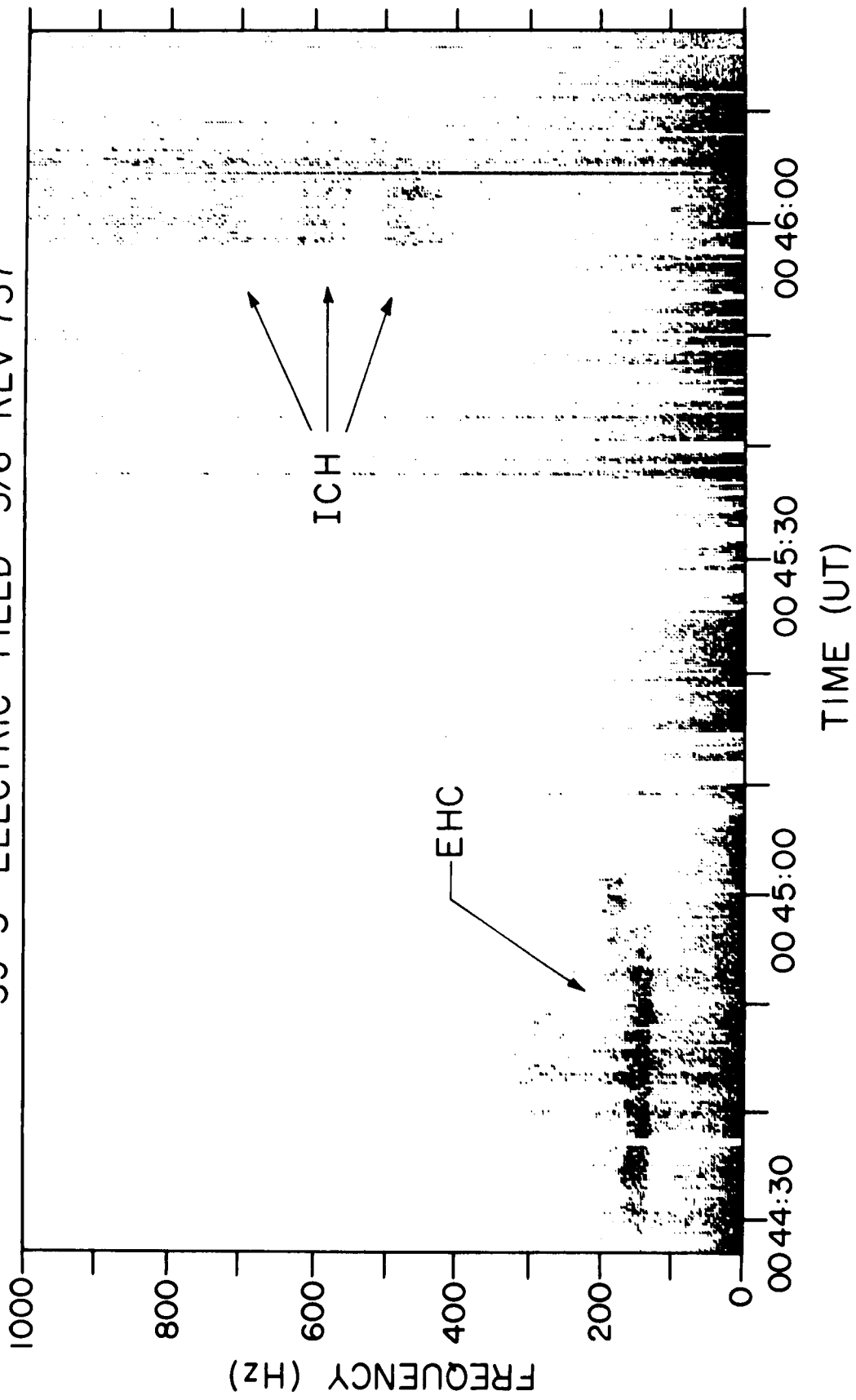


Figure 15

A-G89-221

ISEE-1 APRIL 20, 1981

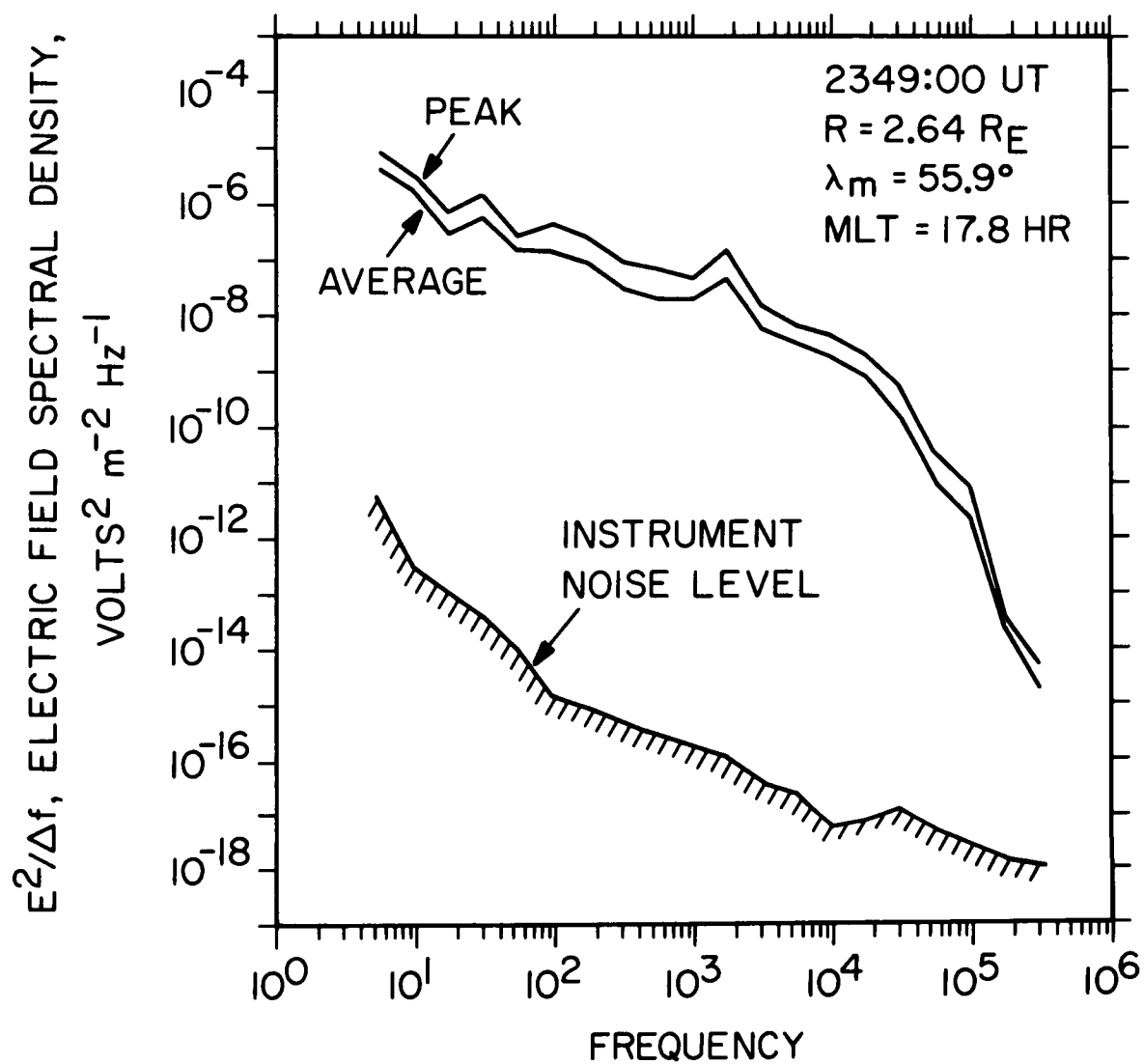


Figure 16